



Your complimentary  
use period has ended.  
Thank you for using  
PDF Complete.

[Click Here to upgrade to  
Unlimited Pages and Expanded Features](#)

Master's thesis

# **Terminally diisocyano functionalized and rotationally restricted biphenyl systems**

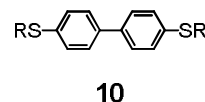
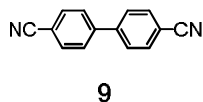
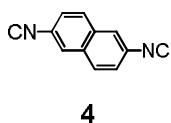
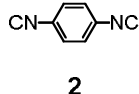
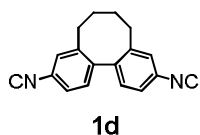
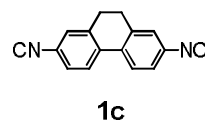
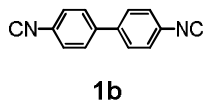
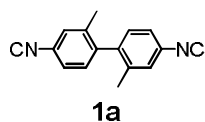
21<sup>st</sup> of January 2010 ó 30<sup>th</sup> of August 2010

Group of Prof. Dr. M. Mayor

Markus Gantenbein

University of Basel

In the last two decades organic molecules, which exhibit molecular electron transport characteristics, have attracted considerable attention. This master's thesis reports a novel universal synthetic route towards diisocyano functionalized biphenyls systems, which are suitable molecules for investigations in this ongoing research area. These biphenyls, bearing a terminal isocyano group in 4,4'-positions, are bridged between 2 and 2' positions by a variable number of methylene groups, giving them a restricted torsion angle between the two phenyl rings. Thus, the biphenyls are model compounds to investigate the influence of  $\pi$ -conjugation, on the molecular transport characteristics. The target molecules are synthesized, starting by converting dibromobiphenyl derivatives into their diamine analogons and followed by a carbon atom insertion in the amino functionality using dichlorocarbene as reagent.



The molecular electron transport characteristics of compounds **1b**, **9** and **10** are investigated in collaboration with the group of *Christian Schönenberger*. They enable a deeper understanding of the influence on the conductance value of the metal-end group bonding in a molecular break junction.

[Click Here to upgrade to  
Unlimited Pages and Expanded Features](#)

1	Introduction.....	1
2	Project.....	3
3	Strategy.....	5
4	Discussion.....	7
4.1	Synthesis of the 4,4'-diisocyano-2,2'-dimethyl-1,1'-biphenyl (1a).....	7
4.1.1	Development of a general pathway towards the target diisocyano-systems .....	7
4.1.2	Pathway b:.....	8
4.1.3	Pathway a.....	9
5	Charge transport through a molecule.....	15
5.1	UV/Vis studies.....	15
5.2	Molecular junction based on diisocyano functionalized biphenyl series.....	17
6	Conclusion and Outlook.....	25
7	Physical principles of electronic conductance.....	28
8	Experimental Part.....	30
8.1	General methods.....	30
8.2	Synthetic part.....	32
9	List of Abbreviations.....	52
10	Literature.....	53

The search for molecular assemblies with promising transport characteristics for electronic devices has been an active field for the past two decades<sup>[1]</sup>. Self-assembled monolayers (SAMs) of thiols on Au(111) surfaces have been examined extensively. This assembly is particularly attractive, because of a strong chemical bond formed between the sulfur and the surface gold atoms. The electron transport characteristics through a single molecule have been studied using mechanically controllable break junctions<sup>[2]</sup> and scanning tunneling microscopy (STM)<sup>[3-5]</sup>.

However, these studies are dominated by two parameters: 1) the formation of a reproducible and stable contact between the molecule and both metal electrodes, and 2) the mismatch between the Fermi level and either the HOMO or LUMO level of the adsorbent molecule. The thiol-gold linkage has been mainly considered for composing molecular electronic devices. Nevertheless, there are still several limitations of thiol-gold surfaces for practical molecular electronic applications. The combination of sulfur and gold yields one of the highest contact barriers for charge transport<sup>[6]</sup>. It is also well known that SAMs of thiols on gold are thermally unstable<sup>[7]</sup>. Furthermore, the stochastic behavior of thiols on gold electrodes, that results from the breakage of the adsorbent molecule-metal contact, has also been observed<sup>[8]</sup>. Therefore, new end groups binding to the Au surface have to be investigated. Since recent studies of *Angelici* and co-workers have shown a strong bond of isocyanides to several metal surfaces, air stable isocyanide self-assembled monolayer (SAM) on Au can be formed, as in the case of thiol SAMs<sup>[9]</sup>. Regarding the smaller energy difference between the Fermi level and the HOMO<sup>[10]</sup>, isocyanides seem to be well-chosen end groups to perform molecular electron transport characteristics.

Biphenyls, as the smallest structures comprising two adjacent benzene rings as individual  $\pi$  systems, are ideal compounds to investigate electronic transport characteristics. Interesting studies have been done to understand the influence of the restricted torsion angle between two phenyl units of a biphenyl system and the conductance value<sup>[11-13]</sup>. The focus of this report is to provide synthetic access to a series of biphenyl model compounds for the investigation of the correlation between the end group and the molecular electron transport characteristics. Considering the studies



*Your complimentary  
use period has ended.  
Thank you for using  
PDF Complete.*

[Click Here to upgrade to  
Unlimited Pages and Expanded Features](#)

who have shown a low and a high conductance value of further investigations are needed to explain such an interaction between two isocyano end groups within a molecular break junction. This report presents two straightforward molecular break junction measurements, which give highly interesting conduction characteristics on two levels separated from each other by about 2 orders of magnitude. We currently hypothesize the formation of a bimolecular dimer in the junction stabilized by Coulomb interaction between two isocyano end groups, as the origin of the lower conducting junction.

The feature of conductance of the molecular junction is contributed to two different physical characteristics, namely the energy matching between the Fermi level of metal electrodes and the influence of the interaction between the conduction orbital of the molecule (HOMO or LUMO) and the bonding end groups on the overall electronic conduction through a molecule. A lot of investigations have been done during the past decade to understand the influence of the molecular structure, i.e. length, conjugation, molecular geometry, conformation, torsion angle, or the bonding end groups<sup>[10-12, 15-20]</sup>. Consequently, different systems exhibiting molecular conductance were investigated by changing the anchor groups. A series of terminally functionalized biphenyls seem to be the suitable model compounds to perform conductance measurements. This project presents a universal synthetic strategy towards terminally isocyano functionalized biphenyl systems. Figure 1 illustrates the diisocyano functionalized target compounds.

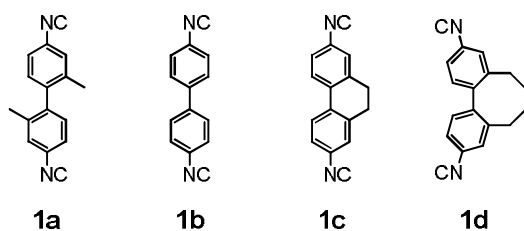


**Figure 1.** Target compounds bearing isocyano anchor groups with increasing torsion angle from **1a** to **1d**.

The goal of this series is to synthesize new compounds with different torsion angles, which are suitable for the examination of the effect of the torsion angle on the conductance. In order to find relations between torsion angle and conductance it is necessary that other parameters, that affect the conductance, remain unchanged. This is why everything but the backbone remains the same throughout this series. The basic idea is to interlink the two phenyl rings through an additional alkyl chain of various lengths bridging the 2,2 $\phi$ -positions<sup>[21]</sup> (Fig. 2). To achieve a reasonably relaxed conformation of the additional alkyl chain, the restricted torsion angle must increase with enlarging alkyl chain. By increasing the number of carbon atoms in the bridging alkyl chain, the restricted torsion angle also increases.

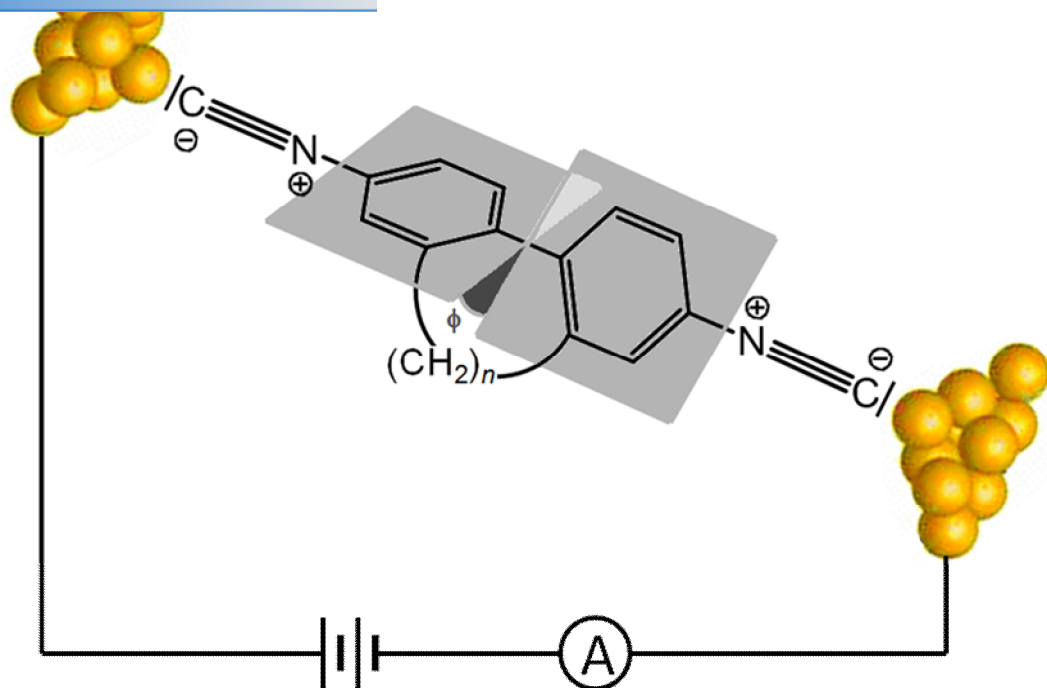
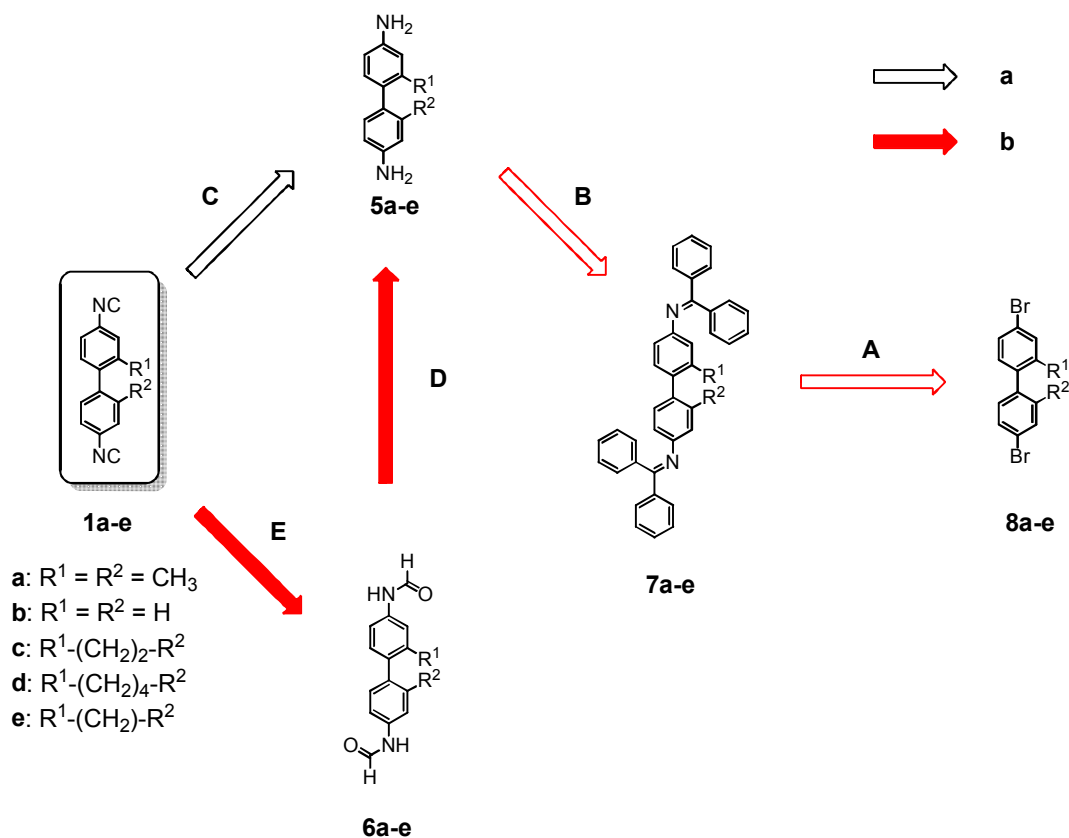


**Figure 2.** Concept illustration of the desired diisocyanide functionalized biphenyls systems building a formation of molecular junction. A single molecule is anchored to electrodes through terminal Au-CN bonds. An alkyl chain with  $n$   $\text{CH}_2$  units interlinks the two phenyl units, adjusting stepwise the interplanar torsion angle.

Molecular transport characteristics are dominated by the bond strength and the difference between the Fermi level and the HOMO or LUMO. Isocyanides bind to transition metals via a strong coordination bond by effective donation to metal and back donation from metals. The strength of the metal-CN bond is comparable to that of the metal-S bond<sup>[14]</sup>. Kubiak and co-workers reported a even smaller energy difference between the Fermi level and the HOMO for the unsubstituted biphenyl molecule anchored by isocyanide groups than for the sulfur groups<sup>[10]</sup>. This strong metal-CN bond and the smaller energy gap are very promising for an increased electron transport through the junction.

With terminally halo substituted biphenyls comprising fixed torsion angles in hand, the synthetic strategy was focused on functional group transformations. The target compounds **1a** to **1d** consist of central biphenyl units of varying  $\pi$ -conjugation, which are substituted with two electron-withdrawing groups in 4 positions and in the 4,4' positions, respectively.



**Scheme 1.** Possible synthetic routes towards the desired biphenyl diisocyanide series. Only pathways used within this report are displayed.

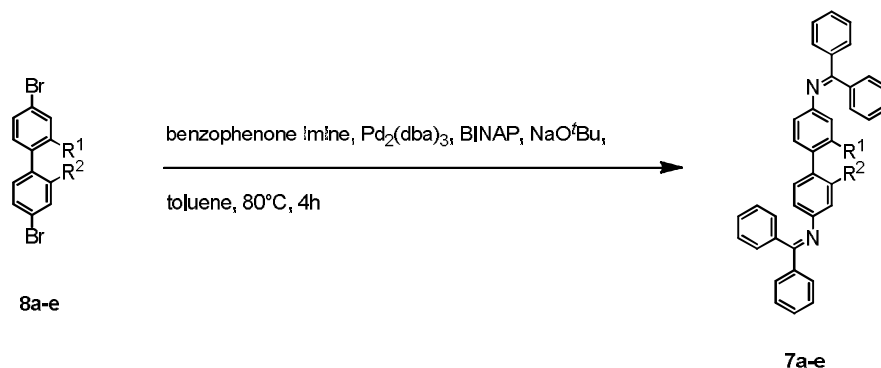
In addition to the normal conditions, like high yielding steps or chemoselectivity, the synthetic pathway should start from the already available 4,4'-dibromobiphenyl derivatives (**8a-e**) or from the commercially available 4,4'-diaminobiphenyl (**5b**) derivative.

ivatives the amine groups in 4 and 4ø position can be analyzed *Hartwig-Buchwald*<sup>[22]</sup> (A) couplings using benzophenone imine, which afterwards can be cleaved to the desired amino functionality (B). If the amine is transformed to the N-arylformamid (D), the dehydrating agent phosphorus oxychloride forms the diisocyanide structure (E). The followed synthetic pathway transforms the primary amine directly to the diisocyanide (C). The amino group of the diamine performs a nucleophilic attack at the dichlorocarbene and forms by  $\beta$ -elemination, followed by  $\alpha$ -elimination the desired target structures.

## 4.1 Synthesis of the 4,4'-diisocyano-2,2'-dimethyl-1,1'-biphenyl (1a)

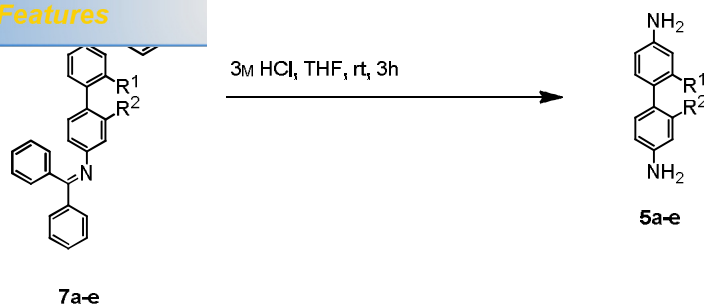
### 4.1.1 Development of a general pathway towards the target diisocyano-systems

With the starting material 4,4'-dibromobiphenyl **8a68e**, benzophenone imine can be used as ammonia synthon. It is reported to be a suitable ammonia source for aryl bromines and triflates, but not for aryl chlorides. Hence, conditions for such a transformation were applied (scheme 2)<sup>[12]</sup>.



**Scheme 2.** Synthesis of **7a67e**.

In this reaction a Pd(0) catalyst in 4 mol%, racemic BINAP, which acts as a bidentate ligand, benzophenone imine as the ammonia synthon and sodium *tert*-butoxide as a strong base were used. The reaction was carried out under inert gas atmosphere, because the formed catalyst-ligand-complex is air-sensitive, and water free due to the base. After 4 hours at 80°C the starting material was consumed, which was monitored by TLC. Products **7a67e** were isolated after purification by recrystallization from methanol. To cleave the imine, the method suggested by *Buchwald* and co-workers (scheme 3) was applied.<sup>[22]</sup>

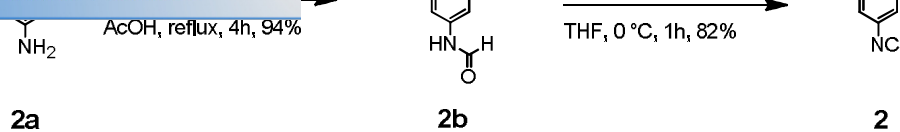


**Scheme 3.** Acidic hydrolysis for the cleavage of the imines (**7a-7e**).

The diimines **7a-7e** were dissolved in THF (0.3 M with respect to the imine) and then acidified with 3M hydrochloric acid. The pure compounds **5a-5e** were isolated by acidic extraction and column chromatography. A yield of 89% was achieved for **5c** and 94% yield for **5d**. Compound **5a** was available from our research group and compounds **5b** and **5e** are commercially available.

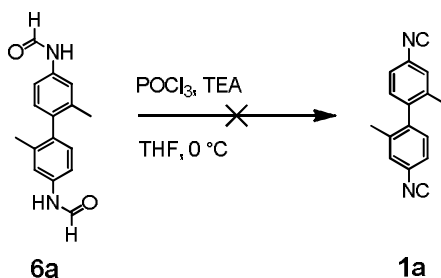
#### 4.1.2 Pathway b:

To prove pathway **b**, a test reaction at the benzene-1,4-diamine **2a** was conducted as a first step. The diamine **2a** was converted to the corresponding the *N,N*ϕ arylldiformamide (**2b**) by using ethyl format and acetic acid as solvent<sup>[23]</sup>. The amine performs a nucleophilic attack on the carbon atom C1 of the ethyl formate, generating a NóC bond. By rearrangement and separating ethanol as a side product, the *N,N*ϕ arylformamide (**2b**) was isolated after filtration. Furthermore, this converted anchor group needed to be transformed to a diisocyanide by a dehydrating reagent in presence of a base<sup>[24]</sup>. In this research triethylamine and phosphorus oxychloride were used as dehydrating reagent to form the diisocyanide<sup>[25]</sup>. After column chromatography and recrystallization in DCM/hexane (1:1), the desired molecule **2** was successfully isolated (scheme 4).



**Scheme 4.** Synthetic pathway **b** using the diamine derivative **2a** as a test molecule.

Unfortunately, no product was isolated after column chromatography by applying these conditions for the dimethyl biphenyl **1a** (scheme 5). The reason for this might be the coordinated oxygen anions of *N,N*- $\phi$ aryldiformamides. Since the anions of the aldehyd-oxygen atom in the biphenyl systems are well stabilized by the mesomeric structure, the acidity of the *N,N*- $\phi$ aryldiformamide decreases drastically in the biphenyl systems<sup>[26]</sup>. Therefore, the reactivity is very low and no 4,4'-diisocyno-2,2'-dimethyl-1,1'-biphenyl (**1a**) was observed by following this pathway. But there was not any further improvement, such as using potassium *t*-butoxide as a stronger base to convert the *N,N*- $\phi$ aryldiformamide successfully to the diisocyanide (**1a**)<sup>[27]</sup>.



**Scheme 5.** Synthesis of the target molecule **1a** using dehydrating reagent phosphorus oxychloride.

### 4.1.3 Pathway a

With the diamine derivatives in hand, the conditions proposed by *Hoffmann* in 1867 were used<sup>[27]</sup> to form the desired diisocyno functionalized biphenyl systems. In this two phase reaction the water phase consists of a 45% potassium hydroxide solution (aq.) and the organic phase of dichloromethane, respectively. The hydroxyl anion in the water phase diffuses to the interphase, whereas the chloroform gets deprotonated. These

organic phase.

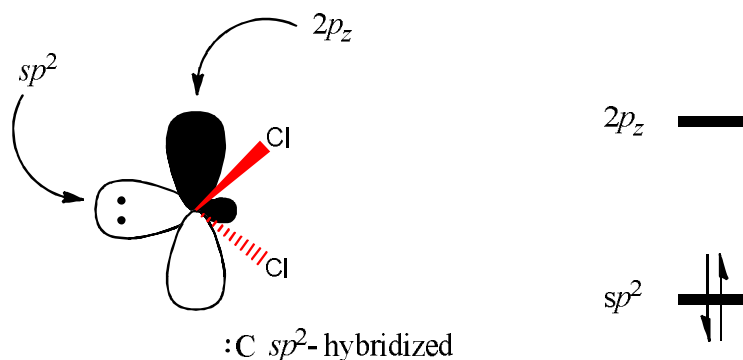
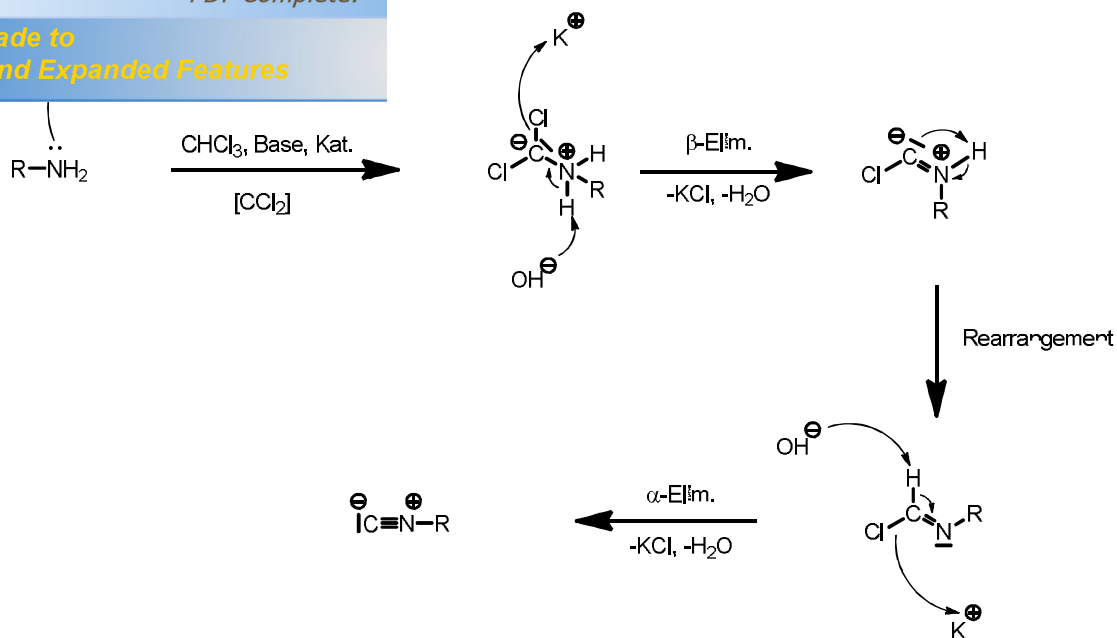


**Figure 3.** Polarized  $\sigma$ -bond with  $\delta^+$  at the carbon atom leads to a singlet state.

Afterwards, the dichlorocarbene is formed by cleaving a chloride atom. Carbenes (figure 3) with substituent like chloride atoms, exerting a strong inductive effect, contain a carbon atom with a charge-deficit and therefore increase electronegativity. This means, that the non-bonding electrons are  $sp^2$  hybridized, as the electrons closer to the core are more stabilized. The singlet carbene operates either as an electrophilic system ( $sp^2$  orbital) or as a nucleophilic system ( $2p_z$  orbital). In this case the amino group of the diamine performs a nucleophilic attack at the dichlorocarbene and forms the carbylamines, by subsequent  $\beta$ -elimination and  $\alpha$ -elimination, which leads to target structures **1a61e** (scheme 6).



**Scheme 6.** Mechanism towards isocyano functionalized molecules using the conditions proposed by Hoffmann.

### Screening of different reaction conditions for synthesizing 4,4'-diisocyano-2,2'-dimethyl-1,1'-biphenyl (**1a**):

By performing the reaction followed by literature<sup>[28]</sup>, a yield of 30% of the desired product **1a** was isolated after purification by column chromatography. The reaction was repeated with an increased number of chloroform equivalents. A conversion to the diisocyanide derivative (**1a**) yielded in 46% after purification. By reason of these unexpected results a screening of different reaction parameter systems was additionally performed. The results are displayed in table 1.

Reaction of **5a** to **1a**.

Reaction conditions	Conc. of diamine <sup>[a]</sup> ( <b>5a</b> )	45% aq. KOH-solution	Phase transfer Catalyst	Chloroform	Reaction time	Yield
a	0.02 [mol/l]	7.0 ml	0.25 mol %	2.0 eqv.	48 hours	66%
b	0.02 [mol/l]	7.0 ml	0.25 mol %	4.0 eqv.	48 hours	66%
c	0.02 [mol/l]	7.0 ml	0.25 mol %	8.0 eqv.	24 hours	52%
d	0.02 [mol/l]	7.0 ml	0.25 mol %	10 eqv.	24 hours	65%
e	0.02 [mol/l]	7.0 ml	1.0 mol %	2.0 eqv.	24 hours	64%
f	0.04 [mol/l]	3.0 ml	0.25 mol %	2.0 eqv.	24 hours	No clean product
g	0.02 [mol/l]	7.0 ml	0.25 mol %	7.0 ml	24 hours	-

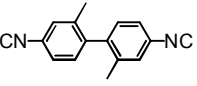
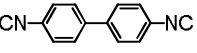
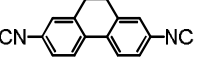
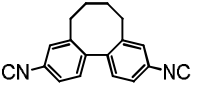
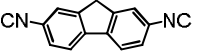
[a] It was assumed that the diamine (**5a**) is absorbed by the organic phase (dichloromethane).

By performing the reaction followed by literature<sup>[28]</sup> and twice as much equivalent of chloroform (entries a and b), a conversion of 66 % was obtained after 48 hours. As the chloroform equivalents were increased to 8, the yield as well as the reaction time decreased. By adding 10 equivalents of chloroform (entry d), the same yield as for entries a and b was obtained, at a shorter reaction time, though. This decrease in reaction time while increasing the chloroform equivalents can be explained statistically. The more chloroform is added, the more dichlorocarbenes are available for the nucleophilic attack of the amine. This higher amount of dichlorocarbenes in the solution increases the possibility of side reactions. Since this reaction is a two phase reaction, the influence of the phase transfer catalyst (entry e) was also tested. By the same amount of chloroform molecules as in entry a, the possibility of forming the dichlorocarbene is increased due to larger amount of phase transfer catalyst. Conclusively, a conversion of 64% at a shorter reaction time was obtained. The increase of concentration raised side reactions, like electrophilic attack of very reactive dichlorocarbene (entry f). By performing in pure chloroform, as the organic phase, no conversion monitored by TLC (entry g) was observed. Nevertheless, a white suspension was obtained pointing at the expected salt formation. To explain this occurrence, a closer look at the reaction mechanism is required. Owing to the formation of the dichlorocarbene an eq. potassium

mination. Upon conversion to the isocyanide, which also  
on, another two eq. potassium chloride are formed. Since  
all the potassium hydroxide molecules were consumed by forming the dichlorocarbene,  
there were no molecules left to perform the conversion to the isocyanide. Less solubility  
in water of the potassium chloride than the potassium hydroxide leads to the observed  
white suspension.

By the screening, the shortest reaction time for such a conversion towards the desired  
diisocyanide derivative **1a** was found, when the reaction was performed adding 10  
equivalents of chloroform or 1 mol % of phase transfer catalyst. All further reactions  
starting from diamine **5b65e** to the resulting diisocyanide derivatives **1b61e** were  
performed by using 10 eq. of chloroform and 1 mol % of phase transfer catalyst within  
the reaction conditions. Yields and selectivities of the other substrates **1b61e** are  
summarized in table 2.

**Table 2.** Conversion of amines **5a65e** to the diisocyanides **1a61e**.  
All yields are isolated yields.

	Product	Yield	Reaction time
<b>1a</b>		65%	24 h
<b>1b</b>		59%	24 h
<b>1c</b>		20%	24 h
<b>1d</b>		33%	24 h
<b>1e</b>		0%	24 h

For the unbridged biphenyl systems **1a** and **1b**, higher yields were obtained than for the  
alkyl chain bridged molecules **1c61e**. We assign these differences to side reactions

chain. The acidity of the benzylic protons in the side  
ed deprotonation disfavoring the transformation to the  
diisocyanides. Therefore, no conversion was obtained for the fluorene (**1e**). The longer  
the bridging alkyl chain the lower the acidity of the benzylic protons. This leads to a  
higher conversion towards diisocyanides for the 86membered ring (**1d**) than for the 66  
membered ring (**1c**).

## 5.1 UV/Vis studies

The correlation between electron absorption characteristics and the interplane torsion angle  $\phi$  was investigated by UV absorption spectroscopy. The UV absorption spectra of the series **1a**–**1d** were measured in hexane at a concentration of  $1.0 \times 10^{-5}$  M. The absorption spectra obtained are displayed in Figure 4.

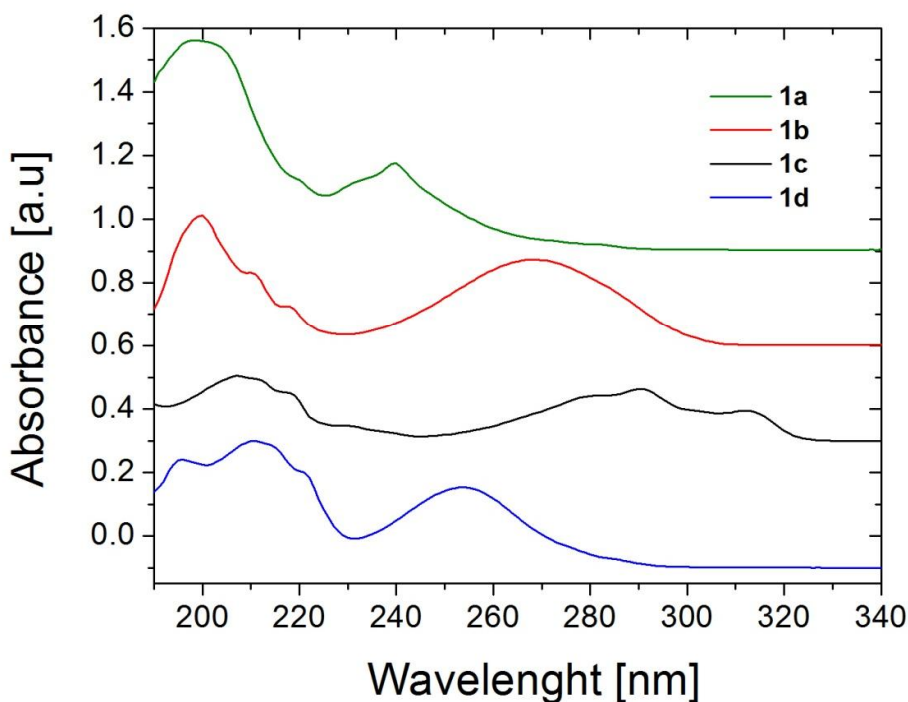


**Figure 4.** UV absorption of the diisocyanides **1a**–**1d** biphenyls in hexane at a concentration of  $1 \cdot 10^{-5}$  M. The absorption spectra are displayed in a stacked mode.

The longest absorption band at around 315 nm, assigned to the  $\alpha$  absorption band, is only observable for the 6-membered ring **1c**. The absorption band between 190 and 230 nm is correlated to the  $\beta$  band. The broad absorption bands of **1a**–**1d** between 230 and 310 nm can be assigned to the  $\rho$  band of the biphenyl subunit. This  $\rho$  band is also called the conjugation band as its position and intensity is reported to reflect the extent of conjugation in the biphenyl core<sup>[29]</sup>. The onset of the  $\rho$  band absorption of each

HOMO-LUMO band gap of the compound under absorption maxima, is reported in Table 3.

**Table 3.** UV adsorption properties of the series **1a**–**1d**.

	$\lambda_{\max}$ [nm]	$\varepsilon$ [L mol <sup>-1</sup> cm <sup>-1</sup> ]	$\lambda_{\text{on}}$ [nm]	HOMO - LUMO band gap [eV]
<b>1a</b>	240	27500	290	4.28
<b>1b</b>	268	27300	310	4.00
<b>1c</b>	290	16300	327	3.79
<b>1d</b>	254	25300	297	4.17

<sup>[a]</sup>  $\lambda_{\max}$  is the wavelength in nm at the maximum of the p band. <sup>[b]</sup>  $\varepsilon$  is the extinction coefficient at  $\lambda_{\max}$  of the p band. <sup>[c]</sup>  $\lambda_{\text{on}}$  is the adsorption onset of the UV spectra.

Within this series of compounds, the expected correlation between the HOMO-LUMO band gap and the restricted torsion angle was observed. The HOMO-LUMO band gap was calculated by using the formula:

$$\text{HOMO-LUMO band gap [eV]} = 1/(\lambda_{\text{on}} \cdot 10^{-7} \text{ nm}) \cdot 8065.5447 \text{ cm}^{-1}$$

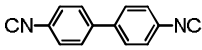
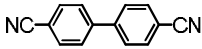
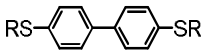
Vonlanthen and co-workers investigated the restricted torsion angle in a biphenyl series with cyanide and thiol as an anchor group<sup>[11, 30]</sup>. Due to the fact that no X-ray solid state structures for our diisocyano functionalized biphenyl series was performed, all the restricted torsion angles between the two phenyl units are assumed to be comparable. Going through the sequences for the molecule **1a** from above, which performs a restricted torsion angle close to 80°, the HOMO-LUMO band gap with the highest energy was obtained. For the unsubstituted biphenyl **1b**, with a restricted torsion angle of around 30°, the HOMO-LUMO gap decreased as expected. Due to the smallest restricted torsion angle (ca. 20°) for molecule **1c**, the smallest energy gap between the HOMO-LUMO was observed. Molecule **1d** performs a torsion angle between the two biphenyl units of about 60°. As expected, the energy of the HOMO-LUMO band gap is higher than for the 6-membered ring (**1c**).

## based on diisocyano functionalized biphenyl

Biphenyls, the smallest structures to comprise two adjacent benzene rings as individual  $\pi$  systems, are ideal model compounds to investigate electronic transport characteristics [31-33]. As it has been reported a strong relation of the restricted torsion angle between these biphenyl systems<sup>[13, 21]</sup> and the anchor group<sup>[14]</sup>, diisocyano functionalized biphenyl derivatives have been used as a model system.

For comparison of transport characteristics of different anchor groups break junction measurements of unsubstituted difunctionalized biphenyl derivatives were performed by *Jan Brunner*, using isocyanide **1b**, cyanide **9** and thiol **10** anchor groups. The molecules which were used for single molecular electron transport measurements are shown in Table 4. The analyzing method of the break junction measurements was followed by the proposed procedure of *Huber* and co-workers<sup>[16]</sup>. The table illustrates further the strategy of the present study. In molecule **9**, the anchor groups include cyanid groups and in molecule **10** the thiol group replaces the isocyanid anchor group. For the other molecules **1a**, **1c** and **1d** no single molecule conductance characteristics have been investigated yet.

**Table 4.** Average single-molecule conductance values  $G_0$ , for molecules **1b**, **9** and **10**, obtained by break junction measurements.

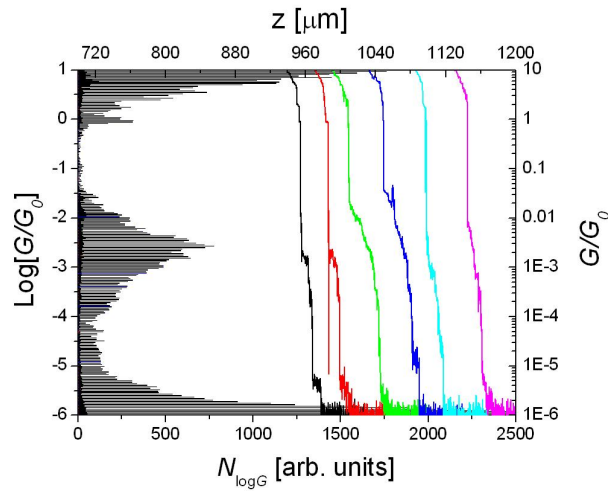
	Molecule	No. Of samples	Conductance ( $G_0$ ) <sup>[b]</sup>
<b>1b</b>		1	$2.1 \cdot 10^{-3}$
<b>9</b>		1	$3.6 \cdot 10^{-5}$
<b>10</b>		1	$1.7 \cdot 10^{-4}$

<sup>[a]</sup> Synthesized with R=Ac; immobilized with R=Au electrodes.

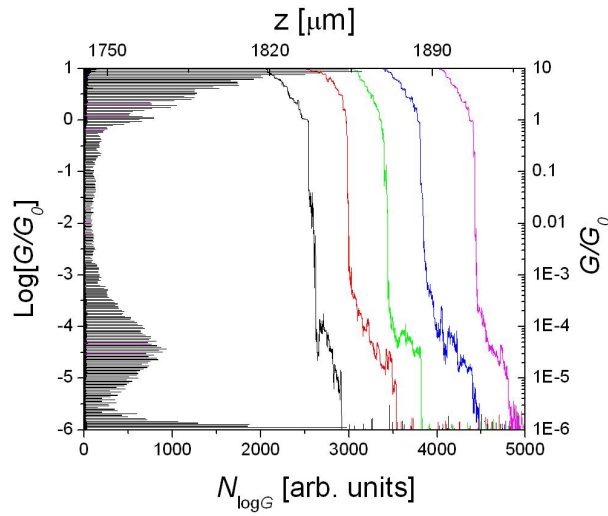
<sup>[b]</sup> Conductance value of molecule **10** has been reported by *Vonlanthen* and co-workers.<sup>[11]</sup>

No electronic transport through a single sulfur anchored biphenyl molecule was obtained in the histogram (Fig. 5). Since some of the up cycles are representing a

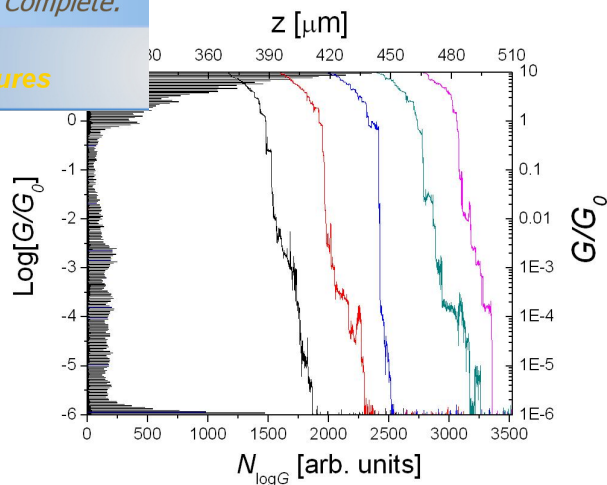
already reported values are found<sup>[11, 31]</sup>, it is not the characteristics.



a)



b)



c)

**Figure 5.** 5 typical single  $G(z)$  curves measured in solvent (1:4 THF:Mesitylene) with added diisocyanide molecules **1b** (a), dicyanide molecules **9** (b) and dithiol molecules **10** (c). The curves are shifted horizontally for clarity. Also shown are histograms ( $N_{\log G}(\log G)$ ) of  $\log(G)$  values obtained from 50 opening curves each.

Going through the sequences, one can see that the conductance value  $G_{\text{peak}}$ , corresponding to the peak position in the log histogram, is reduced for molecule **9** by a factor of 100 compared to the molecule **1b**. This effect is explained by a smaller energy gap between the HOMO and the Fermi level for molecule **1b** and a larger energy gap between LUMO gap and the Fermi level for molecule **9**, respectively.

If the histogram and the open cycles are analyzed more carefully one can see another peak at lower conductance and higher  $z$ . There have been reported several structures performing molecular interactions leading to a second lower conductance peak.<sup>[17]</sup> If there is a lower conductance peak, it can be explained for the same reasons, not for the  $\pi$ - $\pi$  stacking interaction between a pair of molecule but for Coulomb interaction between the anchor groups. This interpretation is supported by the shift of  $G_{\text{peak}}$  to lower values by more than an order of magnitude. In this picture, a reduced  $G$  value is expected because the pair of molecules will be longer than a single diisocyanide molecule anchored between Au electrodes. Therefore, it was investigated a single molecular conductance measurement of a diisocyanide molecule including only one phenyl unit **2** (figure 6).

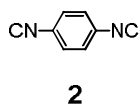


**Figure 6.** Diisocyanobenzene functionalized molecule (2) including only one phenyl unit.

When the isocyanides are attached to the gold surface, the  $\nu(\text{CN})$  bands are observed at much higher frequencies. This increase in  $\nu(\text{CN})$  frequencies for isocyanides attached to gold is generally interpreted as evidence of increased donation of electronic charge from the isocyanide to the gold<sup>[34]</sup>. Decreasing the number of phenyl rings decreases the electron donation to gold, and this results in the effect of lower  $\nu(\text{CN})$  frequencies. The decreased electron donation to gold, in turn, leaves a residual smaller partial positive charge on the isocyanide molecule. The effective smaller partial positive charge causes a rise of the molecular orbital energies. The rise of the isocyanide molecular orbital energies moves  $E_{\text{HOMO}}$  closer to  $E_{\text{Fermi}}$  and  $E_{\text{Fermi}} - E_{\text{HOMO}}$  decreases<sup>[10]</sup>. The obtained results are shown in figure 7.

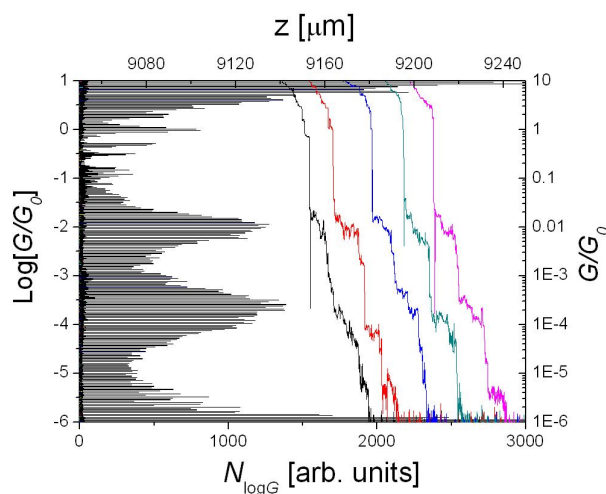


**Figure 7.** 5 typical single  $G(z)$  curves measured in solvent (1:4 THF:Mesitylene) with added diisocyanide molecules 2. The curves are shifted horizontally for clarity. Also shown are histograms ( $N_{\log G}(\log G)$ ) of  $\log(G)$  values obtained from 50 opening curves each.

The histogram of the break junction measurement clearly shows two plateaus, meaning the plateau at a higher conductance peak ( $8.8 \cdot 10^{-3} G_0$ ) is correlated to one molecule in the break junction (Fig. 8 (a)), whereas the plateau at a lower conductance value ( $1.9 \cdot 10^{-4} G_0$ ) is achieved by a pair of molecule (Fig. 8 (b)).

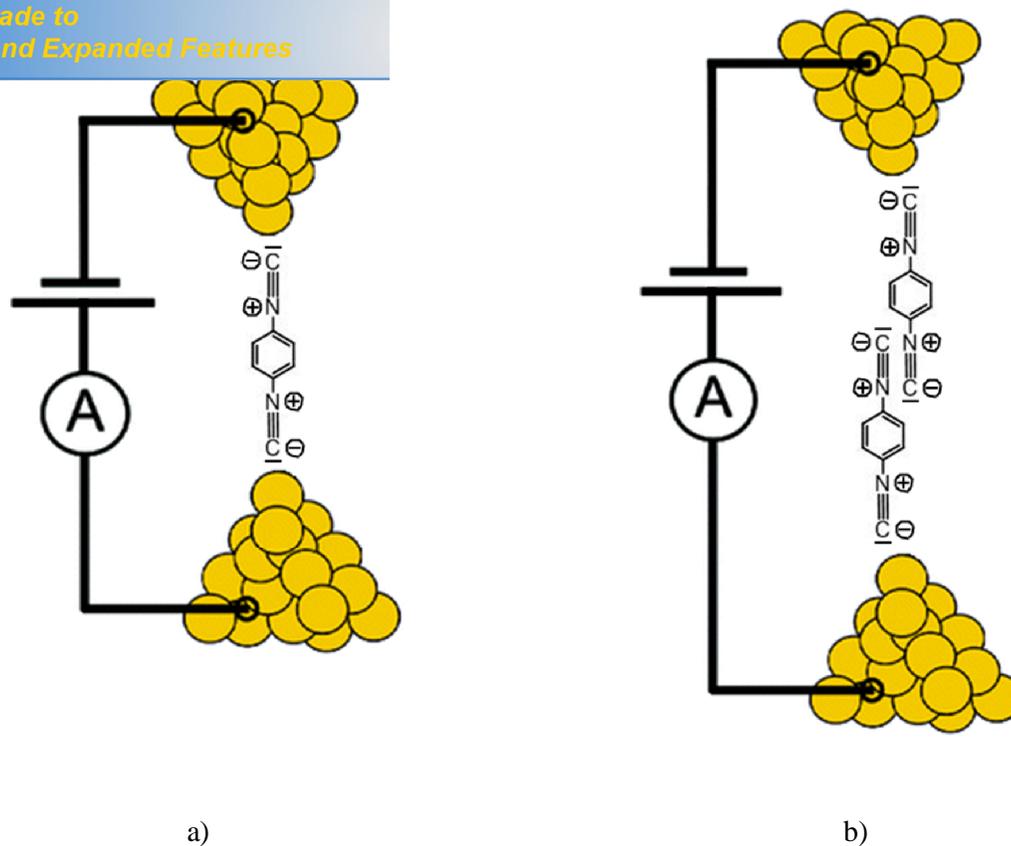


**Figure 8.** Illustration of a) a single diisocyanide biphenyl molecule **2** between two electrodes and b) a possible staggered dipole-dipole stacking configuration of a pair of molecules **2** within which the anchor groups are attached to each other due to Coulomb interactions.

Since the interaction of Coulomb forces only occurs if the isocyanides are included at both sides of the molecule, another straightforward control experiment is necessary to investigate break junction measurements with a monoisocyanide functionalized phenyl unit **3**.

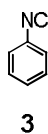
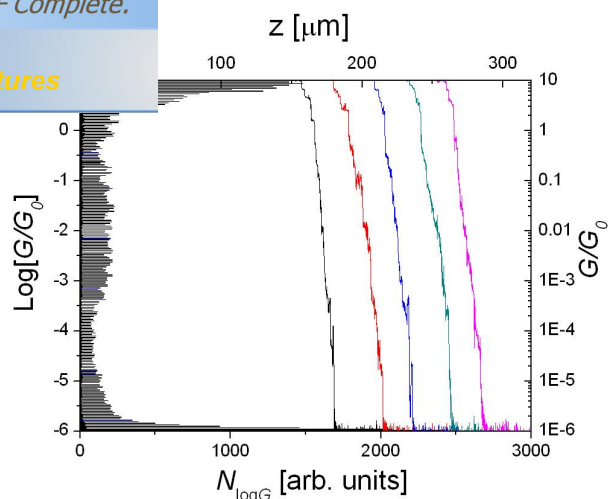
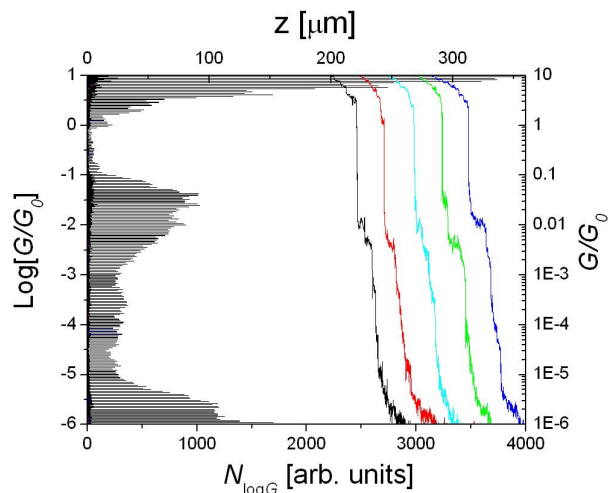


**Figure 9.** Isocyanide functionalized molecule (**3**) including only one phenyl unit.



a)



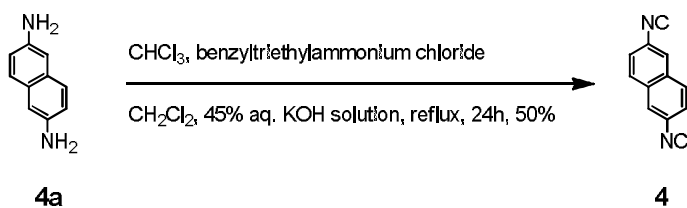
b)

**Figure 10.** 5 typical single  $G(z)$  curves measured in solvent (1:4 THF:Mesitylene) with added monoisocyanide molecules **3** (a) and a mixture of mono- and diisocyanide molecules (1000:1) **3** and **2** (b). The curves are shifted horizontally for clarity. Also shown are histograms ( $N_{\log G}(\log G)$ ) of  $\log(G)$  values obtained from 50 opening curves each.

In figure 10a neither a high nor a low conductance value was obtained for molecule **2**. Since the phenyl unit is only mono functionalized no electron transport properties can be obtained in a molecular break junction, because no junction can just be made of isocyanide. Analyzing figure 10b a conductance value was observed due to performing a molecular junction through the diisocyanide derivative **2**. The much higher concentration of just mono functionalized molecules (**3**) avoids an interaction between

cyano anchor groups. These two control measurements are being due to Coulomb interaction between the formally positively charged nitrogen atom and the formally negatively charged carbon atom.

Since the diisocyno functionalized biphenyl **1b** do not clearly show a low conductance value, another break junction measurement of a molecule with better conjugation and a shorter electrode spacing for the Coulomb dimer was envisaged. Therefore, a diisocyno functionalized naphthalene derivative was synthesized by using the same conditions within pathway **a** (scheme 7).



**Scheme 7.** Synthesis of the target molecule **4** following pathway **b**.

This straightforward experiment will prove whether this Coulomb interaction between two molecules is also strong enough for longer molecules. The results of break junction measurement for diisocyno functionalized naphthalene derivative **4** are shown in figure 11.

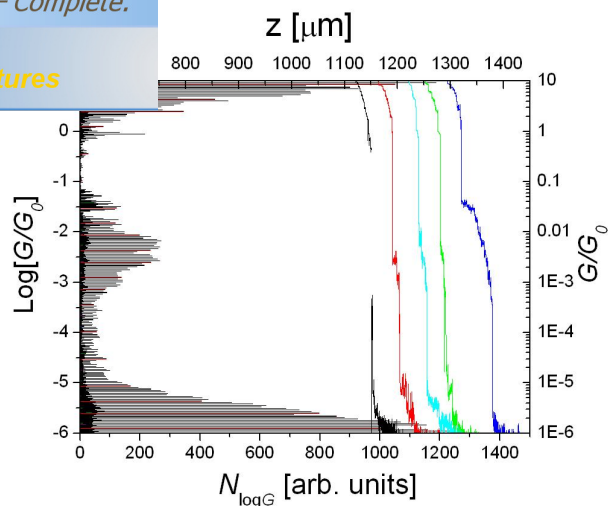
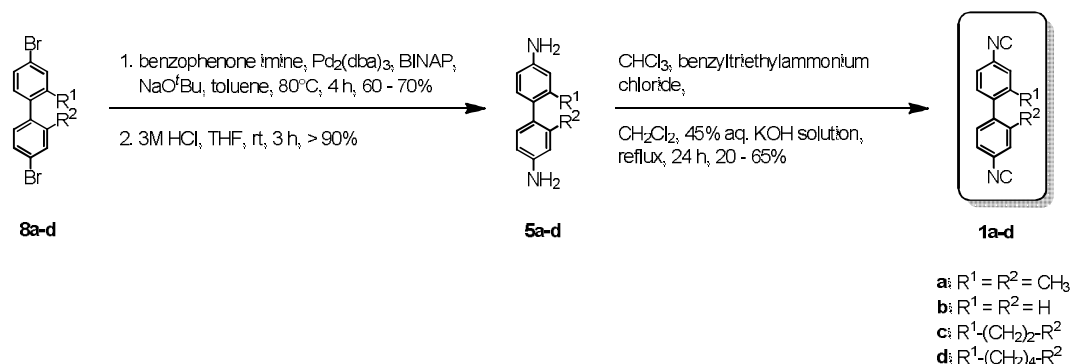


**Figure 11.** 5 typical single  $G(z)$  curves measured in solvent (1:4 THF:Mesitylene) with added diisocyanide molecules **4**. The curves are shifted horizontally for clarity. Also shown are histograms ( $N_{\log G}(\log G)$ ) of  $\log(G)$  values obtained from 50 opening curves each.

The histogram of the diisocyanide functionalized naphthalene molecule **4** reveals a high conductance value at  $4.1 \cdot 10^{-3} G_0$ . Unfortunately, the low conductance value disappears in the noise of the break junction measurement of the setup. The rigid shift towards a higher conductance value of a factor of 2 compared to the diisocyanide biphenyl derivative **1b** is too small. Therefore, the second conductance value, owing to two stacking molecules, cannot be obtained. To prove such interactions between molecules, longer than just one phenyl unit, further investigations have to be done.

## Outlook

Within this thesis the chemistry required to transform dibromides into diisocyanides has been developed. The methodology is of particular interest as it allows the synthesis of model compounds to study the potential of the isocyno group as anchor group in molecular electronics. A series of torsion angle restricted biphenyls with terminal isocyno groups has been synthesized to demonstrate the potential of the method. Conditions for a *Hartwig-Buchwald*<sup>[122]</sup> hetero-cross-coupling reaction to exchange the bromide substituents to amino groups were found, when applied on the 6-membered ring **1c**, using benzophenone imine as an ammonia synthon. These conditions were transferable to all other biphenyl dibromides **8a-d**<sup>[12]</sup>. By availability of terminally halo substituted biphenyl derivatives comprising restricted torsion angles, a first promising synthetic strategy was developed, based on functional group transformations. To provide a variety of diisocyanide derivatives with different torsion angles of the biphenyl moiety, a universal synthetic route towards these molecules was developed. By following the most straightforward synthetic pathway **b**, target molecules **1a-d** were synthesized, starting from the corresponding dibromo derivatives in only three steps (scheme 8). , several interesting and promising results were obtained. With a parameter-screening, promising time reduction and yield enhancement were obtained in this reaction. Further investigations with bases that are better soluble in the solvents could lead to even higher conversion.



**Scheme 8.** Synthetic pathway **b** towards the desired diisocyanide series **1a-d**.

In summary, it can be stated that a universal synthetic route towards the desired diisocyno functionalized systems was developed in order to provide a series of biphenyl including isocyno end groups with defined and fixed torsion angles between

In this report the diisocyanide including one phenyl unit **2**, the diisocyanide **3**, the unsubstituted biphenyl diisocyanide **1b**, as well as the dimethyl **1a**, the six-membered **1c**, the eight-membered **1d**, and the naphthalene **4** derivatives were synthesized. Unfortunately, by applying the conditions to transform the fluorene in the desired diisocyanide **1e**, no conversion was obtained. The very basic condition leads to a deprotonation of the protons at the bridging carbon atom and the highly reactive dichlorocarbene, which is formed within this reaction, increases the side products in this reaction. It has to be achieved another synthetic route for the desired diisocyanide **1e**. Having found a general strategy, derivatives bearing different bridges such as the 7- and 9-membered ring (**1f** and **1g**) derivatives have to be synthesized in order to complete the series. Meanwhile, the building block **11** is available as biphenyls bearing terminal bromide groups in our group (figure 12).

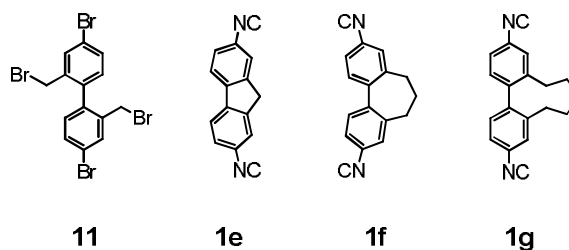


**Figure 12.** Building block of torsion restricted dibromobiphenyls **11** and the desired diisocyanide derivatives **1e-1g** to complete the serie.

Having compound **11** in hand, it is possible to synthesize the desired bridged biphenyl dibromide following the procedure of *Vonlanthen*<sup>[21]</sup>, which allows the application of comparable palladium-catalyzed hetero-cross-coupling reaction conditions to introduce the amino functionalities.

In cooperation with the experimental physicists initial single molecule transport studies were performed. Promising results were obtained by analyzing the break junction measurements<sup>[16]</sup> of **1b**, **2**, **3**, **4** and **9**. Molecular break junction measurements, performed by *Jan Brunner*, member of the group of *Christian Schönenberger*, displayed a dependence of the conductance properties on binding group. Compared to the conductance of **10** ( $1.72 \pm 0.2 \cdot 10^{-4} G_0$ )<sup>[11]</sup>, for compound **9** a very low conductance ( $3.6 \cdot 10^{-5} G_0$ ) was measured, whereas for the diisocyanide compound an even higher conductance ( $2.1 \cdot 10^{-3} G_0$ ) was found than for the dithiol molecule. UV-vis spectra follow the hypothesized trend of an increased  $\pi$ -conjugation in **1c** due to a restricted

While in the case of **1a** a considerable increased torsion due to the steric repulsion of both methyl substituents and leads to a reduced  $\pi$ -conjugation. The break junction measurements nicely illustrate a strong correlation between conductance value and the anchor groups. To estimate the restricted torsion angle with the highest conductance value, break junction measurements of the complete diisocyano functionalized biphenyl series has to be done. To improve the model of the stacking of two molecules other model compounds are required.

## Principles of electronic conductance

To determine the electronic characteristics of molecular junctions, molecules need to be wired between a source and a drain electrode. This has become possible only in the last decade thanks to the development of new experimental techniques that allow the controlled formation of nanometer sized gaps between pairs of metal electrodes<sup>[35, 36]</sup>. Some examples are (a) Transfer printing is used to make top electrodes to self assembled monolayer (SAM)<sup>[37]</sup>; (b) Nanoparticles are taken to bridge the gap which is larger than the molecules<sup>[38]</sup>; and (c) Au colloids can form a 2D arrays of molecular networks.<sup>[39]</sup>

In this report, mechanical controllable break junction (MCBJ) for single molecule measurements was used. An important feature of this technique is the precise control of the gap size at the picometer scale with high mechanical stability, which allows reproducible measurements.

A typical break junction sample used for this report is shown in figure 13. The Au structure is fabricated by e-beam lithography on a flexible spring steel plate substrate onto which a several  $\mu\text{m}$  thick insulating polyimide layer is cast, followed by the evaporation of a 10 nm thin adhesions layer of Ti under an angle of  $\sim 50^\circ$  and the evaporation of 60 nm Au layer perpendicular to the sample. This procedure ensures good adhesion of the Au layer, but avoids Ti in the central region of the bridge due to the angle evaporation. The bridge is typically 150 nm in width and 200-300 nm in length. The bridge is suspended by etching the polyimide on oxygen plasma.

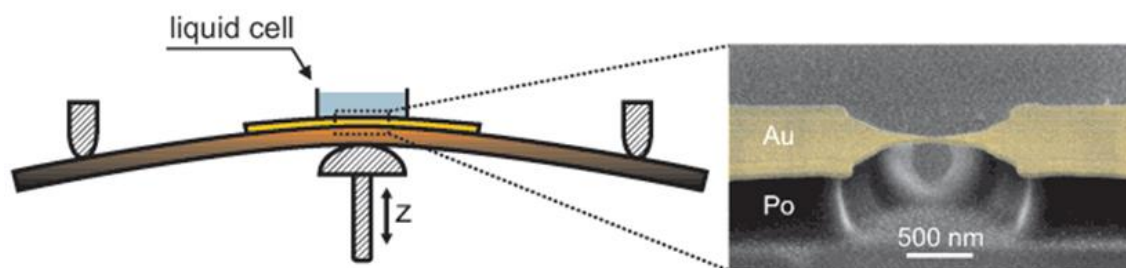


**Figure 13.** Schematics of the MCBJ principle with a liquid cell and a SEM image of the central part of the micro fabricated Au junction.

substrate guarantees a constant immersion of junction in two supports at the periphery and a push rod pressing from below. Bending the substrate results in stretching the suspended Au bridge, which shrinks until it breaks and a gap of size  $d$  forms.

The change in gap  $\Delta d$  is related to the vertical movement of the push rod  $\Delta z$  by an attenuation factor  $a = \Delta d/\Delta z = 1.6 \times 10^{-5}$ <sup>[15]</sup>. The push rod moves at a velocity of  $v_z = 30 \mu\text{m/s}$ , so that the two Au leads separate at  $0.561.2 \text{ nm/s}$ .

For each sample several (up to 200) consecutive open-close cycles have been performed. In forming histograms, the proposed procedure consist of (a) disregarding  $G(z)$  curves that do not present clear plateaus, (b) only using data points that belong to plateaus, instead of taking the whole  $G(z)$  date, (c) only using average values derived from the data points belonging to conductance plateaus, and weighting these by the plateau length, and using conductance jumps<sup>[15]</sup>.

In this work, there have been taken all data and only substracted a background that is adapted to the physics of the problem. This method is as powerful as all the previous ones and, most importantly, it is fully objective. While proceeding, it has been noticed that the conductance must contain a tunneling contribution<sup>[40]</sup>. The tunneling conductance  $G$  is exponentially dependent on the gap distance  $d$ :

$$G \propto \exp(-62\kappa d).$$

Here,  $\kappa = (2m\phi)^{1/2}/\hbar$  is the decay constant and,  $\phi$  the apparent barrier height, and  $m$  the electron mass. Furthermore,  $d = a(z - z_0)$ , where  $a$  is the attenuation factor of the MCBJ<sup>[40]</sup> and  $z_0$  is defined as  $z(d = 0)$ . Rewriting this, we find  $\ln G = -62\kappa a z + \text{constant}$ . It seems therefore much more appropriate to plot histograms of  $\ln G$ , instead of  $G$ .

## 8.1 General methods

### Reagents and solvents:

All chemicals were directly used for the syntheses without purification if nothing else is remarked. Dry solvents were purchased from *Fluka*. The solvents for chromatography and for extractions were not distilled before use. When Schlenk-technic was used, the solvents were degased with argon for several minutes.

### Syntheses:

All reactions with reagents which are easily oxidized or hydrolyzed were performed under an argon atmosphere using Schlenk-technic. Glassware was oven-dried for at least 16 hours or flame-dried and cooled down under an argon flow.

### Analytics and instruments:

**<sup>1</sup>H-Nuclear Magnetic Resonance (NMR):** *Bruker DPX-NMR* (400 MHz), *Bruker BZH-NMR* (250 MHz) instruments were used to record the spectra. Chemical shifts (  $\delta$  ) are reported in ppm relative to residual solvent peaks, and coupling constants,  $J$  ( $\pm 0.1$  Hz) are in Hertz (Hz). NMR solvents were obtained from *Cambridge Isotope Laboratories, Inc.* (Andover, MA, USA). The measurements were performed at room temperature. The multiplicities are written as: s = singlet, d = doublet, t = triplet, q = quartet, quint = quintet and m = multiplet.

**<sup>13</sup>CóNuclear Magnetic Resonance (NMR):** *Bruker DPX-NMR* (101 MHz) was used to record the spectra. Chemical shifts (  $\delta$  ) are reported in ppm relative to residual solvent peaks. The measurements were performed at room temperature. The carbons are classified as: C<sub>q</sub> = quarternary, C<sub>t</sub> = tertiary, C<sub>s</sub> = secondary, C<sub>p</sub> = primary. The peaks

estimations and calculations of increment values, or in measurements.

**Massspectroscopy (MS):** Mass spectra were recorded on an *esquire 3000 plus* (Bruker) for Electron Spray Ionisation (ESI), a *finnigan MAT 95Q* for Electron Impact (EI) or a *Voyager-De<sup>TM</sup> Pro* for MALDI-TOF; measured in m/z (%). EI measurements were done by *H. Nadig*.

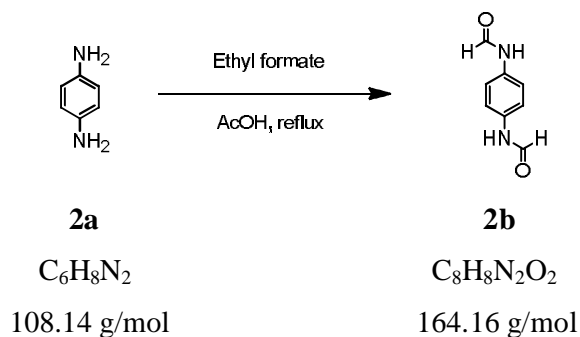
**Elementary Analyses (EA):** The elementary analyses were measured on a *Analysator 240* from Perkin-Elmer by *W. Kirsch*.

**Ultra Violet-Visible Absorptionspectroscopy (UV/Vis):** The UV/Vis spectra were recorded on an *Agilent 8453* Diode Array Spectrophotometer.  $\lambda_{\max}$  (relative intensity, %) was measured in nm.

**Column Chromatography:** For column chromatography *silica gel 60* (40-63  $\mu$ m) from *Fluka* was used.

**Thin Layer Chromatography (TLC):** *Silica gel 60 F<sub>254</sub>* glass plates with a thickness of 0.25 mm from *Merck* were used. The detection was observed with a UV-lamp at 254 nm.

### Synthesis of N, N'-(1,4-phenylene) diformamide (**2b**)<sup>[23]</sup>:



2.60 ml (1.00 eq., 46.2 mmol, 2.80 mg) AcOH and 35.0 ml ethyl formate was added in to a 2-neck-flask charged with 5.00 g (1.00 eq., 46.2 mmol) benzene-1,4-diamine (**2a**). This solution was refluxed until the starting material had been consumed as monitored by TLC. Afterwards, the mixture was cooled to room temperature. The suspension was filtered and washed with ethyl formate. The crude was purified by recrystallization from MeOH/H<sub>2</sub>O to afford 7.15 g (93.5 %) N, N'-(1,4-phenylene) diformamide (**2b**) as a white powder.

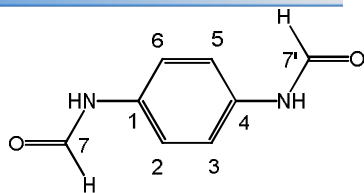
#### Analytical data:

<sup>1</sup>H-NMR (400 MHz, DMSO-D<sub>6</sub>, δ/ppm): 10.13 (s, 2H, H7, H7 $\phi$  (*cis, cis*)), 1H, H7 (*cis, trans*)), 10.07 (d, <sup>3</sup>J<sub>HH</sub> = 11.2 Hz, 1H, H7 $\phi$  (*cis, trans*)), 8.68 (m, 1H, -NH- (*cis, trans*)), 8.22 (m, 2H, -NH- (*cis, cis*)), 1H, -NH- (*cis, trans*)), 7.60  $\delta$  7.46 (m, 4H, H2, H3, H5, H6 (*cis, cis*)), 2H, H2, H5 (*cis, trans*)), 7.18  $\delta$  7.05 (m, 2H, H3, H6 (*cis,trans*)).

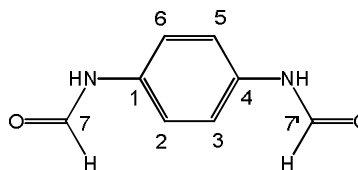
<sup>13</sup>C-NMR (101 MHz, DMSO-D<sub>6</sub>, δ/ppm): 162.5 (C<sub>p</sub>, 1C, C7 $\phi$ ), 159.3 (C<sub>p</sub>, 1C, C7), 134.4  $\delta$  134.0 (C<sub>q</sub>, 2C, C1, C4), 120.2  $\delta$  118.3 (C<sub>t</sub>, 4C, C2, C3, C5, C6).

MS (EI +, 70 eV, m/z (Int. %)): 165.1 (9.6), 164.1 (100).

0.45.



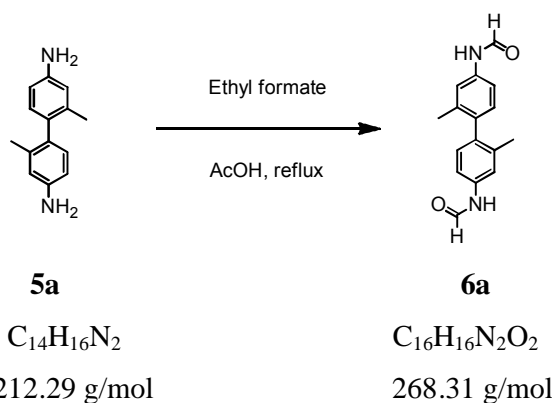
*cis, trans* 6 conformation



*cis, cis* - conformation

### Synthesis of *N,N'*-(2,2'-dimethyl-[1,1'-biphenyl]-4,4'-diyl)diformamide

(**6a**):



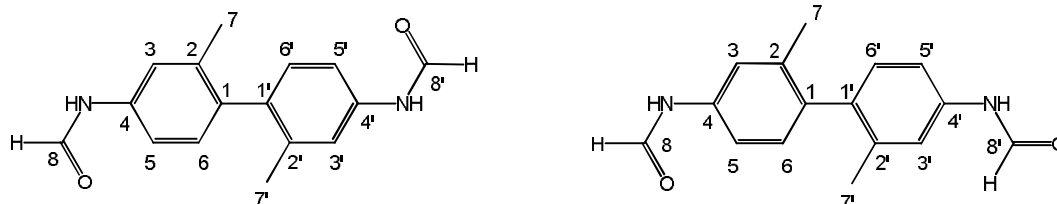
0.200 ml (1.00 eq., 33.4 mmol, 0.200 mg) AcOH and 12.0 ml ethyl formate was added in to a 2-neck-flask charged with 0.710 g (1.00 eq., 33.4 mmol) 2,2'-dimethyl-[1,1'-biphenyl]-4,4'-diamine(**5a**). This solution was refluxed until the starting material had been consumed as monitored by TLC. Afterwards, the mixture was cooled to room temperature. The suspension was filtered and washed with ethyl formate. The crude was purified by recrystallization from <sup>t</sup>BME/hexane to afford 0.520 g (58 %) *N,N'*-(2,2'-dimethyl-[1,1'-biphenyl]-4,4'-diyl)diformamide (**6a**) as a white foam.

**<sup>1</sup>H-NMR** (400 MHz, DMSO-D<sub>6</sub>, δ/ppm): 10.17 (s, 2H, H8, H8 $\phi$  (*cis, cis*)), 1H, H8 (*cis, trans*)), 10.13 (d, <sup>3</sup>J<sub>HH</sub> = 11.0 Hz, 1H, H8 $\phi$  (*cis, trans*)), 8.80 (d, <sup>3</sup>J<sub>HH</sub> = 11.0 Hz, 1H, -NH- (*cis, trans*)), 8.27 (d, <sup>3</sup>J<sub>HH</sub> = 1.9 Hz, 2H, -NH- (*cis, cis*)), 1H, -NH- (*cis, trans*)), 7.51 (d, <sup>3</sup>J<sub>HH</sub> = 1.9 Hz, 2H, H3, H3 $\phi$  (*cis, cis*)), 1H, H3 (*cis, trans*)), 7.43 (dd, <sup>3</sup>J<sub>HH</sub> = 8.2, 2.1 Hz, 2H, H3 $\phi$ H5 (*cis, trans*)), 1H, H5, (*cis, cis*)) 7.12 (d, <sup>3</sup>J<sub>HH</sub> = 1.9 Hz, 1H, H5 $\phi$  (*cis, cis*)), 7.04 (dd, <sup>3</sup>J<sub>HH</sub> = 8.2 Hz, <sup>4</sup>J<sub>HH</sub> = 2.2 Hz, 1H, H5 $\phi$  (*cis, trans*)), 6.98 (d, <sup>3</sup>J<sub>HH</sub> = 8.2 Hz, 2H, H6, H6 $\phi$  (*cis, cis*)), 2H, H6, H6 $\phi$  (*cis, trans*)), 1.95 (s, 6H, H7, H7 $\phi$  (*cis, cis*)), H7, H7 $\phi$  (*cis, trans*)).

**<sup>13</sup>C-NMR** (101 MHz, CDCl<sub>3</sub>, δ/ppm): 162.8 (C<sub>p</sub>, 1C, C8), 159.2 (C<sub>p</sub>, 1C, C8 $\phi$ ), 130.9 (C<sub>q</sub>, 2C, C2, C2 $\phi$ ), 130.2 (C<sub>q</sub>, 2C, C1, C1 $\phi$ ), 121.4 (C<sub>q</sub>, 2C, C4, C4 $\phi$ ), 120.4 (C<sub>t</sub>, 2C, C3, C3 $\phi$ ), 117.4 (C<sub>t</sub>, 2C, C6, C6 $\phi$ ), 116.2 (C<sub>t</sub>, 2C, C5, C5 $\phi$ ), 20.1 (C<sub>p</sub>, 2C, C7 $\phi$ , C7 $\phi$ ).

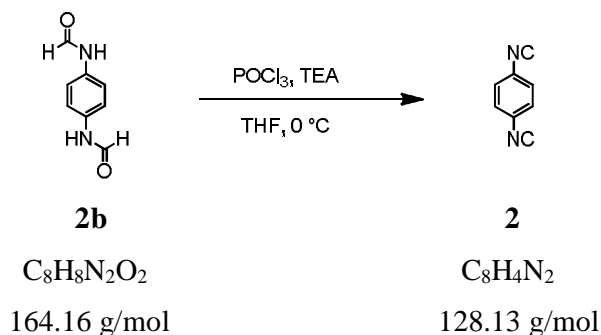
**MS** (EI +, 70 eV, m/z (Int. %)): 268.1 (100), 269.1 (18), 270.1 (1.9).

**R<sub>f</sub>** (SiO<sub>2</sub>; EtOAc + 5% TEA) = 0.55.



*cis, trans*  $\phi$  conformation

1,4-diformamide (2b)<sup>[25]</sup>:



500 mg (1.00 eq., 30.5 mmol) N, N'-(1,4-phenylene) diformamide (**2b**) was added to a solution of 2.60 ml TEA (12.5 ml, 6.00 eq., 1.90 mg) in 12.5 ml THF. The solution was cooled at 0 °C, while 0.70 ml (1.20 eq., 36.6 mmol, 1.10 mg) phosphoryl oxochloride was added drop wise. The reaction mixture was stirred until the starting material had been consumed as monitored by TLC. After the reaction was completed, saturated Na<sub>2</sub>CO<sub>3</sub> aqueous solution was added at 0 °C to quench the reaction. The product was extracted with <sup>t</sup>BME, dried over sodium sulfate, filtered and concentrated *in vacuo*. The orange crude was purified by column chromatography (SiO<sub>2</sub>, hexane:EtOAc 100:1 ó 10:1) and recrystallization in DCM/hexane to afford 320 mg (82%) 1,4-diisocyanobenzene (**2**).

**Analytical data:**

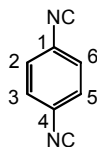
<sup>1</sup>H-NMR (400 MHz, CDCl<sub>3</sub>, δ/ppm): 7.44 (s, 4H).

<sup>13</sup>C-NMR (101 MHz, CDCl<sub>3</sub>, δ/ppm): 167.7 (CN-), 127.8 (C<sub>q</sub>, 2C, C1, C4, C<sub>t</sub>, 4C, C2, C2ø, C3, C3ø).

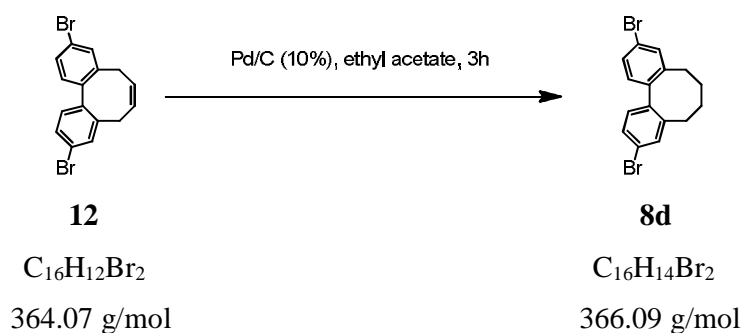
MS (EI +, 70 eV, m/z (Int. %)): 128 (100), 129 (8.7).

R<sub>f</sub> (SiO<sub>2</sub>; hexane:EtOAc 4:1) = 0.42.

IR ν(CN-): 2130.2 cm<sup>-1</sup>.



**Synthesis of (Z) 3,10-dibromo-5,6,7,8-tetrahydrodibenzo[a,c][8]annulene (8d)<sup>[21]</sup>:**



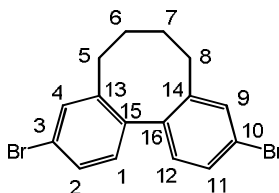
1.84 g (1.00 eq., 5.06 mmol) of (Z)-3,10-dibromo-5,8-dihydrodibenzo[a,c][8]annulene (**12**) in 82.0 ml ethyl acetate was given in a oven-dried 250 ml-flask. To this mixture 135 mg (10 % Pd/C, 2.50 mol%, 0.130 mmol) palladium on charcoal was added and the black suspension was stirred vigorously under hydrogen (1 atm) for 3h. The suspension was filtered through a silica pad, washed with ethyl acetate and the solvent was concentrated *in vacuo*. 1.81 g (97%) of 3,10-dibromo-5,6,7,8-tetrahydrodibenzo[a,c][8]annulene (**8d**) was collected a white solid.

**Analytical data:**

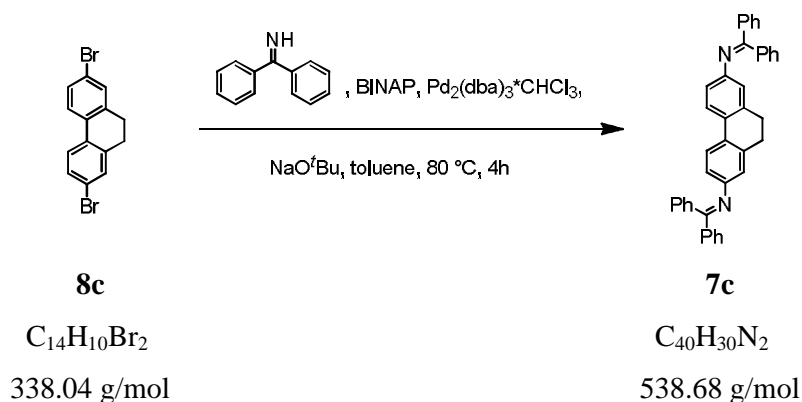
<sup>1</sup>H-NMR (400 MHz, CDCl<sub>3</sub>, δ/ppm): 7.42 (d, <sup>3</sup>J<sub>HH</sub> = 2.1 Hz, 2H, H1, H12), 7.73 (dd, <sup>3</sup>J<sub>HH</sub> = 8.1 Hz, <sup>4</sup>J<sub>HH</sub> = 2.1 Hz, 2H, H2, H11), 7.07 (d, <sup>3</sup>J<sub>HH</sub> = 8.1 Hz, 2H, H4, H9), 2.68 (dd, <sup>2</sup>J<sub>HH</sub> = 13.4 Hz, <sup>3</sup>J<sub>HH</sub> = 8.5 Hz, 2H, H5, H8), 2.11 ó 2.05 (m, 4H, H5, H6, H7, H8), 1.52 ó 1.46 (m, 2H, H6, H7).

R<sub>f</sub> (SiO<sub>2</sub>; hexane:CH<sub>2</sub>Cl<sub>2</sub> 95:5) = 0.75.

ed to literature<sup>[21]</sup>.



### Synthesis of $N^2,N^7$ -bis(diphenylmethylene)-9,10-dihydrophenanthrene-2,7-diamine (**7c**)<sup>[12]</sup>:



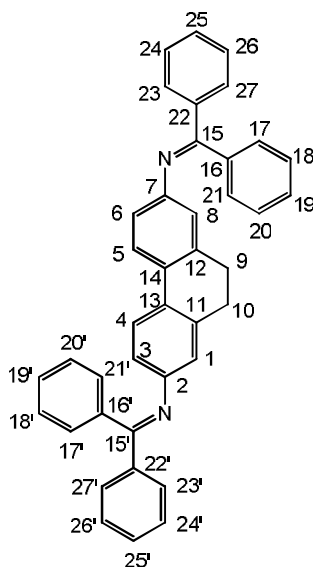
According to procedure<sup>[12]</sup> 49.0 mg (4.00 mol%, 0.0473 mmol)  $Pd_2(dba)_3 \cdot CHCl_3$  and 88.5 mg (12.0 mol%, 0.142 mmol) BINAP in 7.4 ml degassed toluene and 400 mg (1.00 eq., 1.18 mmol) 2,7-dibromo-9,10-dihydrophenanthrene (**8c**), 318.3 mg (2.80 eq., 3.31 mmol)  $NaO^tBu$  and 0.480 ml (2.40 eq., 2.84 mmol, 514 mg) benzophenone imine were used. 584 mg (64%)  $N^2,N^7$ -bis(diphenylmethylene)-9,10-dihydrophenanthrene-2,7-diamine (**7c**) was isolated after recrystallization from MeOH as a pale yellow powder.

[Click Here to upgrade to  
Unlimited Pages and Expanded Features](#)

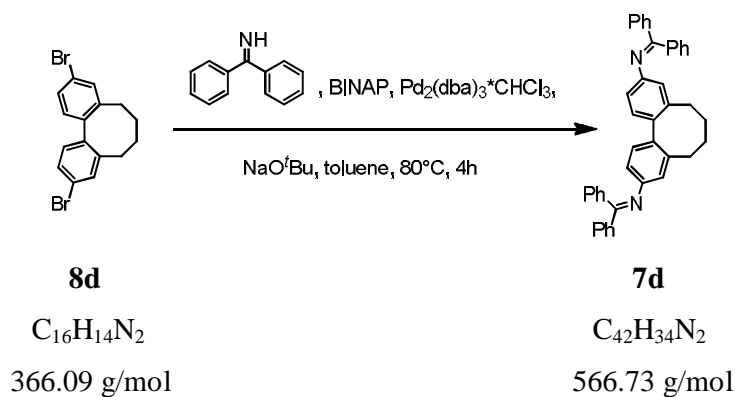
$^1\text{H-NMR}$  (400 MHz,  $\text{CDCl}_3$ ,  $\delta/\text{ppm}$ ): 7.74 (d,  $^3J_{\text{HH}} = 7.1$  Hz, 4H, H17, H17 $\alpha$ , H27, H27 $\phi$ ), 7.46 (tt,  $^3J_{\text{HH}} = 7.2$  Hz,  $^4J_{\text{HH}} = 2.4$  Hz, 2H, H19, H19 $\phi$ ), 7.42  $\delta$  7.37 (m, 6H, H4, H4 $\alpha$ , H18, H18 $\alpha$ , H20, H20 $\phi$ ), 7.29  $\delta$  7.23 (m, 6H, H24, H24 $\alpha$ , H25, H125 $\alpha$ , H26, H26 $\phi$ ), 7.17  $\delta$  7.13 (m, 4H, H23, H23 $\alpha$ , H21, H21 $\phi$ ), 6.62 (d,  $^2J_{\text{HH}} = 2.1$  Hz, 2H, H13, H14 $\phi$ ), 6.55 (dd,  $^3J_{\text{HH}} = 8.2$  Hz,  $^4J_{\text{HH}} = 2.2$  Hz, 2H, H6, H3), 2.64 (s, 4H, H9, H10).

$R_f$  ( $\text{SiO}_2$ ; hexane:EtOAc 5:1) = 0.47.

The analytical data was accorded to literature<sup>[12]</sup>.



(diphenylmethylene)-5,6,7,8  
annulene-3,10-diamine (**5d**)<sup>[12]</sup>:



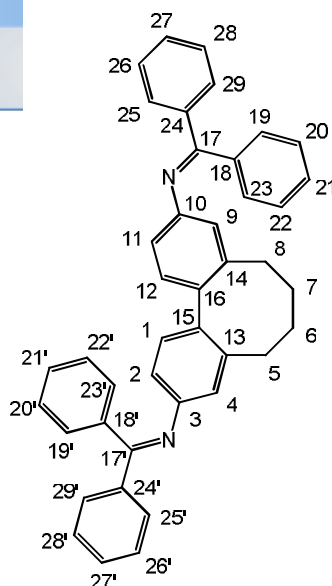
According to procedure<sup>[12]</sup> 34.1 mg (4.00 mol%, 0.0330 mmol) Pd<sub>2</sub>(dba)<sub>3</sub> · CHCl<sub>3</sub> and 62.0 mg (12.0 mol%, 0.0990 mmol) BINAP in 5.20 ml degassed toluene and 300 mg (1.00 eq., 0.820 mmol) 3,10-dibromo-5,6,7,8-tetrahydrodibenzo[a,c][8]annulene (**8d**), 221 mg (2.80 eq., 2.30 mmol) NaO<sup>t</sup>Bu and 0.330 ml (2.40 eq., 1.97 mmol, 356 mg) benzophenone imine were used. 267 mg (58%) *N*<sup>3</sup>,*N*<sup>10</sup>-bis(diphenylmethylene)-5,6,7,8-tetrahydrodibenzo[a,c][8]annulene-3,10-diamine (**7d**) was isolated after recrystallization as a pale yellow powder.

**Analytical data:**

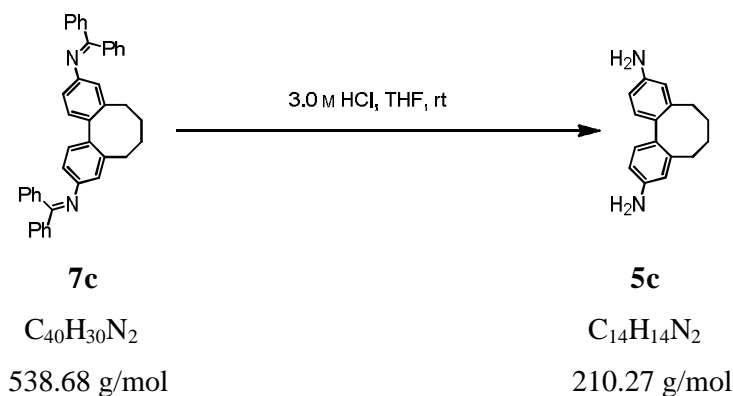
<sup>1</sup>H-NMR (400 MHz, CDCl<sub>3</sub>, δ/ppm): 7.77 (d, <sup>3</sup>J<sub>HH</sub> = 7.0 Hz, 4H, H19, H23, H19 $\alpha$ , H23 $\phi$ ), 7.47 (tt, <sup>3</sup>J<sub>HH</sub> = 7.2 Hz, <sup>4</sup>J<sub>HH</sub> = 2.4 Hz, 2H, H21, H21 $\phi$ ), 7.44  $\delta$  7.38 (m, 6H, H1, H1 $\alpha$ , H20, H21 $\alpha$ , H22, H22 $\phi$ ), 7.30  $\delta$  7.21 (m, 6H, H26, H27, H26 $\alpha$ , H27 $\alpha$ , H28, H28 $\phi$ ), 7.16  $\delta$  7.10 (m, 4H, H25, H25 $\alpha$ , H29, H29 $\phi$ ), 6.97 (d, <sup>2</sup>J<sub>HH</sub> = 2.1 Hz, 2H, H4, H4 $\phi$ ), 6.53 (dd, <sup>3</sup>J<sub>HH</sub> = 8.2 Hz, <sup>4</sup>J<sub>HH</sub> = 2.2 Hz, 2H, H2, H2 $\phi$ ), 2.41 (dd, <sup>2</sup>J<sub>HH</sub> = 13.1 Hz, <sup>3</sup>J<sub>HH</sub> = 8.3 Hz, 2H, H5, H8), 1.89  $\delta$  1.76 (m, 4H, H5, H8, H6, H7), 1.15  $\delta$  1.05 (m, 2H, H6, H7).

*R*<sub>f</sub> (SiO<sub>2</sub>; hexane:EtOAc 5:1) = 0.34.

The analytical data was accorded to literature<sup>[12]</sup>.



### Synthesis of 9,10-dihydrophenanthrene-2,7-diamine (**5c**)<sup>[12]</sup>:

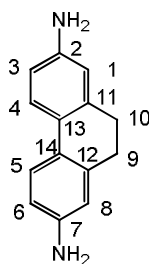


Following a literature known protocol<sup>[12]</sup>, 407 mg (1.00 eq., 0.755 mmol) diimine **7c** was dissolved in 5.00 ml THF, adding 1.50 ml 3 M aq. HCl. The pale yellow reaction mixture was stirred at rt until the starting material was consumed as monitored by TLC. Afterwards the solution was partitioned between 0.5 M aq. HCl and 2:1 hexane/EtOAc. The organic layer was extracted three times with 0.5 M aq. HCl and the combined aqueous layers made alkaline with 1 M aq. NaOH. The brown liquid was extracted with dichloromethane, dried over sodium sulfate, filtered and concentrated *in vacuo*. After purification by column chromatography (SiO<sub>2</sub>, hexane:EtOAc 1:1, 5% NEt<sub>3</sub>) 140 mg (89%) of diamine **5c** was isolated as a yellow solid.

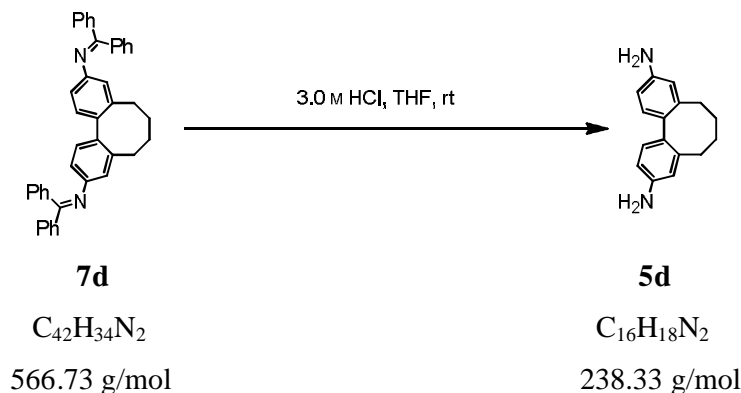
$^1\text{H-NMR}$  (400 MHz,  $\text{CDCl}_3$ ,  $\delta/\text{ppm}$ ): 7.45 (d,  $^3J_{\text{HH}} = 8.2$  Hz, 2H, H4, H5), 6.60 (dd,  $^3J_{\text{HH}} = 8.2$  Hz,  $^4J_{\text{HH}} = 2.4$  Hz, 2H, H3, H6), 6.54 (d,  $^4J_{\text{HH}} = 2.4$  Hz, 2H, H1, H8), 3.61 (s (broad), 4H,  $-\text{NH}_2$ ), 2.75 (s, 2H, H9, H10).

$R_f$  ( $\text{SiO}_2$ ; hexane:EtOAc 1:5, 5%  $\text{NEt}_3$ ) = 0.43.

The analytical data was accorded to literature<sup>[12]</sup>.



### Synthesis of 5,6,7,8-tetrahydrodibenzo[a,c][8]annulene-3,10-diamine (2d)<sup>[12]</sup>:



Following the general procedure<sup>[12]</sup>, 267 mg (1.00 eq., 0.470 mmol) diimine **7d** was dissolved in 3.20 ml THF, adding 1.00 ml 3 M aq. HCl. The pale yellow reaction mixture was stirred at rt until the starting material was consumed as monitored by TLC. Afterwards the solution was partitioned between 0.5 M aq. HCl and 2:1 hexane/EtOAc.

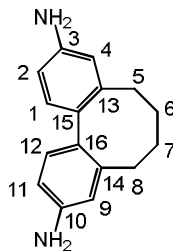
and three times with 0.5 M aq. HCl and the combined  
with 1 M aq. NaOH. The brown liquid was extracted with  
dichloromethane, dried over sodium sulfate, filtered and concentrated *in vacuo*. After  
purification by column chromatography (SiO<sub>2</sub>, hexane:EtOAc 1:1, 5% NEt<sub>3</sub>) 107 mg  
(94%) of diamine **5d** was isolated as a yellow solid.

**Analytical data:**

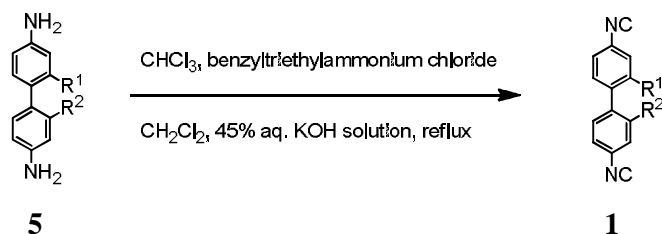
<sup>1</sup>H-NMR (400 MHz, CDCl<sub>3</sub>, δ/ppm): 7.02 (d, <sup>3</sup>J<sub>HH</sub> = 8.2 Hz, 2H, H1, H12), 6.61 ó 6.54  
(m, 4H, H2, H4,H9, H11), 3.62 (s (broad), 4H, -NH<sub>2</sub>), 2.57 (dd, <sup>2</sup>J<sub>HH</sub> = 13.2, <sup>3</sup>J<sub>HH</sub> = 8.2  
Hz, 2H, H5, H8), 2.16 ó 1.97 (m, 4H, H5, H6, H7, H8), 1.51 ó 1.42 (m, 2H, H6, H7).

*R<sub>f</sub>* (SiO<sub>2</sub>; hexane:EtOAc 1:1, 5% NEt<sub>3</sub>) = 0.22.

The analytical data was accorded to literature<sup>[12]</sup>.

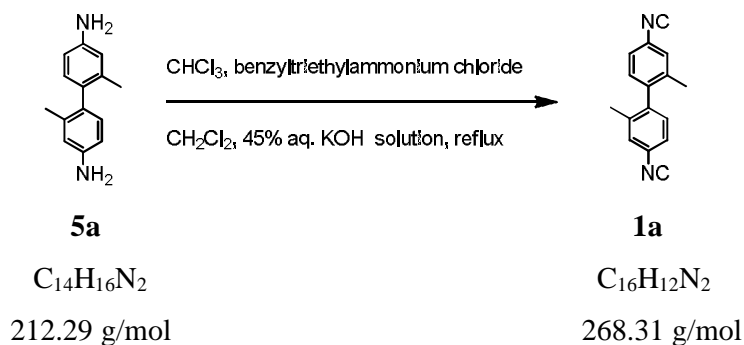


Procedure A: Synthesis of 4,4'-diisocyano-1,1'-



The diaminebiphenyl (**5**) was dissolved in a mixture  $\text{CH}_2\text{Cl}_2$ :45% aq. KOH solution (1:1). To the biphasic mixture, benzyltriethylammonium chloride and chloroform were added. The reaction mixture was heated at reflux until the starting material had been consumed as monitored by TLC. After cooling to rt the mixture was transferred to a separatory funnel diluted with water, and washed twice with water and once with brine. The organic layer was dried over magnesium sulphate, and the solvent was removed by evaporation. The product was further purified by column chromatography ( $\text{SiO}_2$ , cyclohexane: $\text{CH}_2\text{Cl}_2$  1:9) to afford 4,4'-diisocyano-1,1'-biphenyl (**4**) as a white solid. For elementary analysis the product (**4**) was additionally purified by vacuum sublimation.

Synthesis of 4,4'-diisocyano-2,2'-dimethyl-1,1'-biphenyl (**1a**)<sup>[41]</sup>:



Procedure A was followed using 25.0 mg (1.00 eq., 0.140 mmol) 2,2'-dimethyl-[1,1'-biphenyl]-4,4'-diamine (**5a**) was dissolved in 7.00 ml  $\text{CH}_2\text{Cl}_2$  and 7.00 ml 45% aq. KOH solution. To the biphasic mixture benzyltriethylammonium chloride (3.19 mg, 1.00 mol%) and 0.125 ml (10.0 eq, 1.40 mmol, 0.170 g) chloroform was added. The product

ography (SiO<sub>2</sub>, cyclohexane:CH<sub>2</sub>Cl<sub>2</sub> 1:9) to afford 21.3  
'-dimethyl-1,1'-biphenyl (**1a**) as a white solid. For  
elementary analysis the product (**1a**) was additionally purified by vacuum sublimation  
(4 · 10<sup>-2</sup> mbar) at 80 °C.

**Analytical data:**

<sup>1</sup>H-NMR (400 MHz, CDCl<sub>3</sub>, δ/ppm): 7.58 (d, <sup>4</sup>J<sub>HH</sub> = 1.6 Hz, 2H, H6, H6 $\emptyset$ ), 7.46 (dd, <sup>3</sup>J<sub>HH</sub> = 8.1 Hz, <sup>4</sup>J<sub>HH</sub> = 1.9 Hz, 2H, H3, H3 $\emptyset$ ), 7.20 (d, <sup>3</sup>J<sub>HH</sub> = 8.1 Hz, 2H, H5, H5 $\emptyset$ ), 1.99 (s, 6H, H7, H7 $\emptyset$ ).

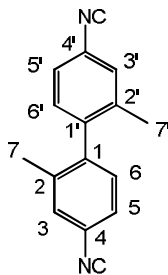
<sup>13</sup>C-NMR (101 MHz, CDCl<sub>3</sub>, δ/ppm): 164.4 (CN-), 141.3 (C<sub>q</sub>, 2C, C1, C1 $\emptyset$ ), 137.7 (C<sub>q</sub>, 2C, C2, C2 $\emptyset$ ), 130.2 (C<sub>t</sub>, 2C, C6, C6 $\emptyset$ ), 128.0 (C<sub>t</sub>, 2C, C3, C3 $\emptyset$ ), 124.0 (C<sub>q</sub>, 2C, C4, C4 $\emptyset$ ), 19.7 (C<sub>s</sub>, 2C, C7, C7 $\emptyset$ ).

MS (EI +, 70 eV, M/z (Int. %)): 232.1 (100), 233.1 (18), 234.1 (1.4).

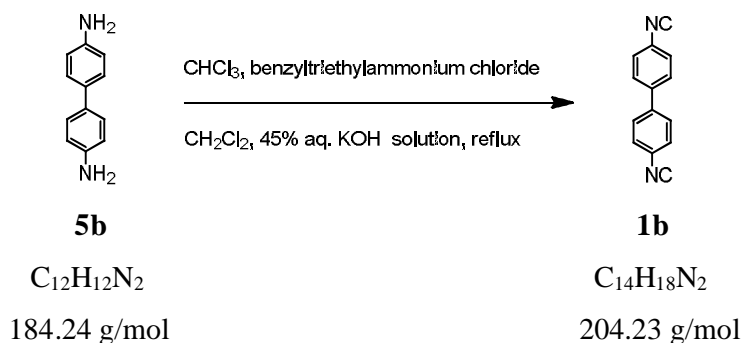
EA: found:	C = 82.43	H = 5.48	N = 11.95
Calc.:	C = 82.73	H = 5.21	N = 12.06

R<sub>f</sub> (SiO<sub>2</sub>; hexane:EtOAc 4:1) = 0.51.

IR ν(CN-): 2117.7 cm<sup>-1</sup>.



4,4'-diisocyanato-1,1'-biphenyl (**1b**):



According to procedure A 141 mg (1.00 eq., 0.760 mmol) benzidine (**5b**) was dissolved in 37.0 ml  $\text{CH}_2\text{Cl}_2$  and 37.0 ml 45% aq. KOH solution. To the biphasic mixture benzyltriethylammonium chloride (17.3 mg, 1.00 mol%) and 0.610 ml (10.0 eq, 7.60 mmol, 0.907 g) chloroform was added. The product was purified by column chromatography ( $\text{SiO}_2$ , cyclohexane: $\text{CH}_2\text{Cl}_2$  1:9) to afford 91.2 mg (59%) 4,4'-diisocyanato-1,1'-biphenyl (**1b**) as a white solid. For elementary analysis the product (**1b**) was additionally purified by vacuum sublimation ( $4 \cdot 10^{-2}$  mbar) at 80 °C.

**Analytical data:**

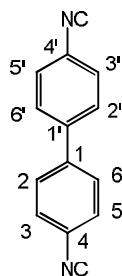
**$^1\text{H-NMR}$**  (400 MHz,  $\text{CDCl}_3$ ,  $\delta$ /ppm): 7.62  $\delta$  7.54 (m, 4H, H2, H2 $\phi$ , H6, H6 $\phi$ ), 7.52  $\delta$  7.43 (m, 4H, H3, H3 $\phi$ , H5, H5 $\phi$ ).

**$^{13}\text{C-NMR}$**  (101 MHz,  $\text{CDCl}_3$ ,  $\delta$ /ppm): 165.6 (CN-), 140.6 ( $\text{C}_q$ , 2C, C1, C1 $\phi$ ), 128.3 ( $\text{C}_t$ , 4C, C3, C5, C3 $\phi$ , C5 $\phi$ ), 127.2 ( $\text{C}_t$ , 4C, C2, C6, C2 $\phi$ , C6 $\phi$ ,  $\text{C}_q$ , 2C, C4, C4 $\phi$ ).

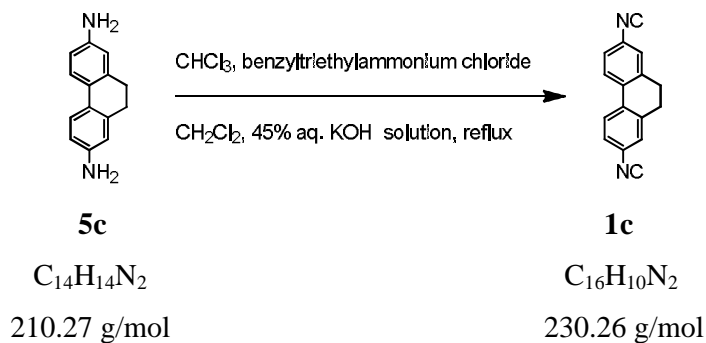
**MS** (EI +, 70 eV, m/z (Int. %)): 204.07 (100), 205.07 (15.9), 206.08 (1.1).

**$R_f$**  ( $\text{SiO}_2$ ; c-hexane: $\text{CH}_2\text{Cl}_2$  1:9) = 0.36.

**IR**  $\nu$ (CN-): 2125.4  $\text{cm}^{-1}$ .



### Synthesis of 2,7-diisocyanato-9,10-dihydrophenanthrene (**1c**):



According to procedure A 140 mg (1.00 eq., 0.666 mmol) 9,10-dihydrophenanthrene-2,7-diamine (**5c**) was dissolved in 32.0 ml  $\text{CH}_2\text{Cl}_2$  and 32.0 ml 45% aq. KOH solution. To the biphasic mixture benzyltriethylammonium chloride (15.2 mg, 1 mol%) and 0.540 ml (10.0 eq, 6.66 mmol, 0.795 g) chloroform was added. The product was purified by column chromatography ( $\text{SiO}_2$ , cyclohexane: $\text{CH}_2\text{Cl}_2$  1:9) to afford 30.7 mg (20%) 2,7-diisocyanato-9,10-dihydrophenanthrene (**1c**) as a white solid. For elementary analysis the product (**1c**) was additionally purified by vacuum sublimation ( $5 \cdot 10^{-2}$  mbar) at 100 °C.

#### Analytical data:

$^1\text{H-NMR}$  (400 MHz,  $\text{CDCl}_3$ ,  $\delta/\text{ppm}$ ): 7.71 (d,  $^3J_{\text{HH}} = 8.3$  Hz, 2H, H4, H5), 7.34 (dd,  $^3J_{\text{HH}} = 8.3$  Hz,  $^4J_{\text{HH}} = 2.0$  Hz, 2H, H3, H6), 7.22 (d,  $^4J_{\text{HH}} = 1.9$  Hz, 2H, H1, H8), 2.88 (s, 4H, H9, H10).

$\delta$ /ppm): 165.1 (CN-), 139.0 (C<sub>q</sub>, 2C, C13, C14), 134.3 (2C, C4, C5), 125.4 (C<sub>t</sub>, 2C, C3, C6), 125.2 (C<sub>t</sub>, 2C, C1, C8, C<sub>q</sub>, 2C, C2, C7), 28.4 (C<sub>s</sub>, 2C, C9, C10).

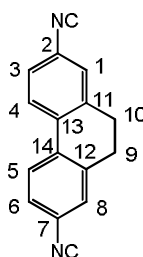
MS (EI +, 70 eV, m/z (Int. %)): 230.1 (100.0), 231.1 (17.4), 232.1 (1.4).

EA: found: C = 82.75 H = 5.55 N = 10.67

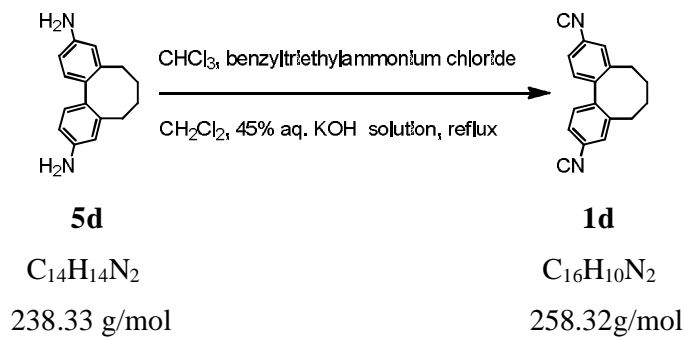
Calc.: C = 83.46 H = 4.38 N = 12.17

$R_f$  (SiO<sub>2</sub>; hexane:CH<sub>2</sub>Cl<sub>2</sub> 1:9) = 0.49.

IR  $\nu$ (CN-): 2129.3 cm<sup>-1</sup>.



### Synthesis of 3,10-diisocyano-5,6,7,8-tetrahydrodibenzo[a,c][8]annulene (1d):



According to procedure A 107 mg (1.00 eq., 0.448 mmol) 5,6,7,8-tetrahydrodibenzo[a,c][8]annulene-3,10-diamine (**5d**) was dissolved in 22.0 ml CH<sub>2</sub>Cl<sub>2</sub>

ution. To the biphasic mixture benzyltriethylammonium and 0.360 ml (10.0 eq, 4.48 mmol, 0.535 g) chloroform was added. The product was purified by column chromatography (SiO<sub>2</sub>, cyclohexane:CH<sub>2</sub>Cl<sub>2</sub> 1:9) to afford 38.2 mg (33%) 3,10-diisocyano-5,6,7,8-tetrahydrodibenzo[a,c][8]annulene (**1d**) as a white solid. For elementary analysis the product (**1d**) was additionally purified by vacuum sublimation ( $6 \cdot 10^{-2}$  mbar) at 100 °C.

**Analytical data:**

**<sup>1</sup>H-NMR** (400 MHz, CDCl<sub>3</sub>, δ/ppm): 7.32 (d, <sup>4</sup>J<sub>HH</sub> = 1.6 Hz, 2H, H1, H12), 7.28 (dd, <sup>3</sup>J<sub>HH</sub> = 8.1 Hz, <sup>4</sup>J<sub>HH</sub> = 1.9 Hz, 2H, H2, H11), 7.22 (d, <sup>3</sup>J<sub>HH</sub> = 8.0 Hz, 2H, H4, H9), 2.73 (dd, <sup>2</sup>J<sub>HH</sub> = 13.6 Hz, <sup>3</sup>J<sub>HH</sub> = 8.5 Hz, 2H, H5, H8), 2.14 ó 2.04 (m, 4H, H5, H6, H7, H8), 1.51 ó 1.43 (m, 2H, H6, H7).

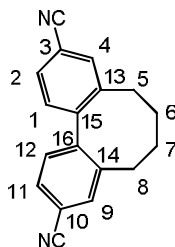
**<sup>13</sup>C-NMR** (101 MHz, CDCl<sub>3</sub>, δ/ppm): 164.5 (CN-), 144.4 (C<sub>q</sub>, 2C, C15, C16), 140.3 (C<sub>q</sub>, 2C, C13, C14), 130.0 (C<sub>t</sub>, 2C, C1, C12), 127.5 (C<sub>t</sub>, 2C, C11, C2), 124.0 (C<sub>t</sub>, 2C, C4, C9, C<sub>q</sub>, 2C, C3, C10), 32.4 (C<sub>s</sub>, 2C, C5, C8), 29.1 (C<sub>s</sub>, 2C, C6, C7).

**MS** (EI+, 70 eV, m/z (Int. %)): 258.12 (100.0), 259.12 (19.6), 260.12 (1.9).

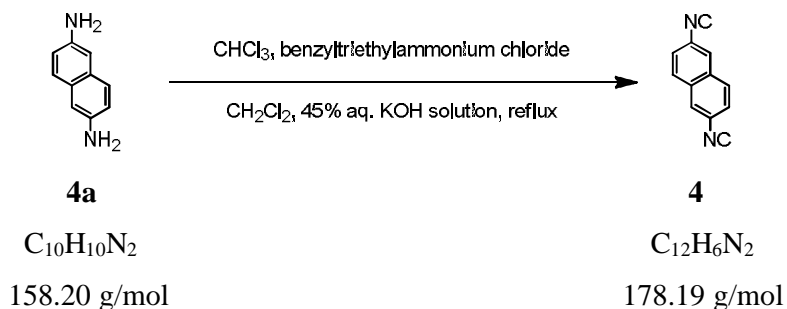
**EA:** found: C = 82.75 H = 5.55 N = 10.67  
Calc.: C = 83.46 H = 4.38 N = 12.17

**R<sub>f</sub>** (SiO<sub>2</sub>; hexane:CH<sub>2</sub>Cl<sub>2</sub> 1:9) = 0.57.

**IR** ν(CN-): 2119.6 cm<sup>-1</sup>.



## 2,6-Diisocyanonaphthalene (4):



According to procedure A 140 mg (1.00 eq., 0.885 mmol) 2,6-diaminonaphthalene (**4a**) was dissolved in 44.0 ml  $\text{CH}_2\text{Cl}_2$  and 44.0 ml 45% aq. KOH solution. To the biphasic mixture benzyltriethylammonium chloride (20.2 mg, 1 mol%) and 0.710 ml (10.0 eq, 8.85 mmol, 1.05 g) chloroform was added. The product was purified by column chromatography ( $\text{SiO}_2$ , cyclohexane: $\text{CH}_2\text{Cl}_2$  1:9) to afford 78.9 mg (50%) 2,6-diisocyanonaphthalene (**4**) as a pale yellow solid. For elementary analysis the product (**4**) was additionally purified by vacuum sublimation ( $7 \cdot 10^{-2}$  mbar) at 100 °C.

### Analytical data:

$^1\text{H-NMR}$  (400 MHz,  $\text{CDCl}_3$ ,  $\delta/\text{ppm}$ ): 7.92 (d,  $^4J_{\text{HH}} = 1.4$  Hz, 2H, H1, H5), 7.89 (d,  $^3J_{\text{HH}} = 8.6$  Hz, 2H, H8, H4), 7.52 (dd,  $^3J_{\text{HH}} = 8.7$  Hz,  $^4J_{\text{HH}} = 1.7$  Hz, 2H, H3, H7).

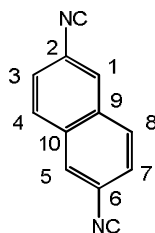
$^{13}\text{C-NMR}$  (101 MHz,  $\text{CDCl}_3$ ,  $\delta/\text{ppm}$ ): 166.2 (CN-), 132.4 ( $\text{C}_q$ , 2C, C9, C10), 130.0 ( $\text{C}_t$ , 2C, C4, C8), 125.9 ( $\text{C}_t$ , 2C, C1, C5), 125.3 ( $\text{C}_t$ , 2C, C3, C7,  $\text{C}_q$ , 2C, C2, C6).

**MS** (EI +, 70 eV,  $m/z$  (Int. %)): 178.1 (100), 179.1 (13.0).

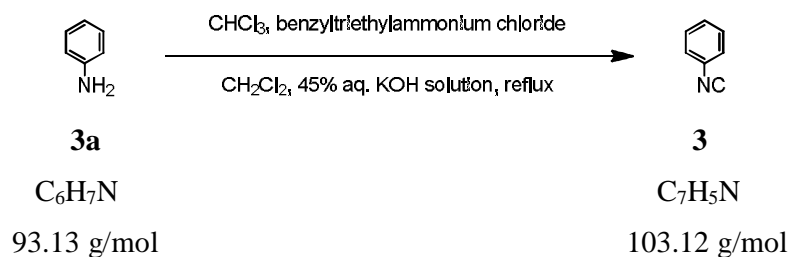
<b>EA: found:</b>	C = 80.53	H = 3.55	N = 15.41
Calc.:	C = 80.89	H = 3.39	N = 15.72

$R_f$  ( $\text{SiO}_2$ ; hexane: $\text{CH}_2\text{Cl}_2$  1:9) = 0.75.

**IR**  $\nu(\text{CN}^-)$ : 2130.2  $\text{cm}^{-1}$ .



### Synthesis of isocyanobenzene (**3**):



According to procedure A 1.00 ml (1.00 eq., 11.0 mmol, 1.02 g) aniline (**3a**) was dissolved in 550 ml  $CH_2Cl_2$  and 550 ml 45% aq. KOH solution. To the biphasic mixture benzyltriethylammonium chloride (125 mg, 1 mol%) and 4.44 ml (5.00 eq, 55.0 mmol, 6.57 g) chloroform was added. The product was purified by column chromatography ( $SiO_2$ , cyclohexane: $CH_2Cl_2$  1:9) to afford 74.7 mg (71%) isocyanobenzene (**3**) as dark blue liquid. For elementary analysis the product (**3**) was additionally purified by distillation at 160 °C.

#### Analytical data:

$^1H$ -NMR (400 MHz,  $CDCl_3$ ,  $\delta$ /ppm): 7.41  $\delta$  7.36 (m, 5H, H2, H3, H4, H5, H6).

$^{13}C$ -NMR (101 MHz,  $CDCl_3$ ,  $\delta$ /ppm): 163.8 (CN-), 129.31 ( $C_q$ , 1C, C1), 126.3 ( $C_t$ , 5C, C2, C3, C4, C5, C6).

MS (EI +, 70 eV, m/z (Int. %)): 103.1 (100.0), 103.1 (7.6).

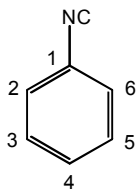
EA: found: C = 80.85 H = 5.12 N = 13.38

[Click Here to upgrade to  
Unlimited Pages and Expanded Features](#)

$$R_f = 4.89 \quad N = 13.58$$

$$R_f (\text{SiO}_2; \text{hexane:CH}_2\text{Cl}_2 \text{ 1:9}) = 0.71.$$

$$\text{IR } \nu(\text{CN}^-): 2126.4 \text{ cm}^{-1}.$$



AcOH	acetic acid	h	hour
aq.	aqueous	HOMO	highest occupied molecular orbital
BINAP	2,2'- bis(diphenylphosphi no)-1,1'-binaphthyl	HPA	heteropolyanion
cat.	catalytic	LUMO	lowest occupied molecular orbital
conc.	concentrated	Me	methyl
min	minute	<i>p</i>	para
NEt <sub>3</sub>	triethyl amine	rt	room temperature
DMSO	dimethyl sulfoxide	TLC	thin layer chromatography
eq.	equivalent	THF	tetrahydrofuran
Et	ethyl	CDCl <sub>3</sub>	Chloroform
Et <sub>2</sub> O	diethyl ether	MeOH	Methanol
EtOAc	ethyl acetate		

## 10 Literature

- [1] Wang, W. Y.; Lee, T.; Reed, M. A., *Reports on Progress in Physics*, (2005) **68**, 523.
- [2] Reed, M. A.; Zhou, C.; Muller, C. J.; Burgin, T. P.; Tour, J. M., *Science*, (1997) **278**, 252.
- [3] Xiao, X. Y.; Xu, B. Q.; Tao, N. J., *Nano Letters*, (2004) **4**, 267.
- [4] Ulrich, J.; Esrail, D.; Pontius, W.; Venkataraman, L.; Millar, D.; Doerrer, L. H., *Journal of Physical Chemistry B*, (2006) **110**, 2462.
- [5] Xu, B. Q.; Tao, N. J. J., *Science*, (2003) **301**, 1221.
- [6] Seminario, J. M.; De la Cruz, C. E.; Derosa, P. A., *Journal of the American Chemical Society*, (2001) **123**, 5616.
- [7] Delamarche, E.; Michel, B.; Kang, H.; Gerber, C., *Langmuir*, (1994) **10**, 4103.
- [8] Ramachandran, G. K.; Hopson, T. J.; Rawlett, A. M.; Nagahara, L. A.; Primak, A.; Lindsay, S. M., *Science*, (2003) **300**, 1413.
- [9] Angelici, R. J.; Lazar, M., *Inorganic Chemistry*, (2008) **47**, 9155.
- [10] Hong, S.; Reifenberger, R.; Tian, W.; Datta, S.; Henderson, J. I.; Kubiak, C. P., *Superlattices and Microstructures*, (2000) **28**, 289.
- [11] Vonlanthen, D.; Mishchenko, A.; Elbing, M.; Neuburger, M.; Wandlowski, T.; Mayor, M., *Angewandte Chemie-International Edition*, (2009) **48**, 8886.
- [12] Rotzler, J.; Vonlanthen, D.; Barsella, A.; Boeglin, A.; Fort, A.; Mayor, M., *European Journal of Organic Chemistry*, (2010), 1096.
- [13] Venkataraman, L.; Park, Y. S.; Whalley, A. C.; Nuckolls, C.; Hybertsen, M. S.; Steigerwald, M. L., *Nano Letters*, (2007) **7**, 502.
- [14] Kiguchi, M.; Miura, S.; Hara, K.; Sawamura, M.; Murakoshi, K., *Applied Physics Letters*, (2006) **89**,
- [15] Gonzalez, M. T.; Brunner, J.; Huber, R.; Wu, S. M.; Schonenberger, C.; Calame, M., *New Journal of Physics*, (2008) **10**,
- [16] Huber, R.; Gonzalez, M. T.; Wu, S.; Langer, M.; Grunder, S.; Horhoiu, V.; Mayor, M.; Bryce, M. R.; Wang, C. S.; Jitchati, R.; Schonenberger, C.; Calame, M., *Journal of the American Chemical Society*, (2008) **130**, 1080.
- [17] Wu, S. M.; Gonzalez, M. T.; Huber, R.; Grunder, S.; Mayor, M.; Schonenberger, C.; Calame, M., *Nature Nanotechnology*, (2008) **3**, 569.
- [18] Kushmerick, J. G.; Holt, D. B.; Pollack, S. K.; Ratner, M. A.; Yang, J. C.; Schull, T. L.; Naciri, J.; Moore, M. H.; Shashidhar, R., *Journal of the American Chemical Society*, (2002) **124**, 10654.
- [19] Lee, M. H.; Speyer, G.; Sankey, O. F., *Physica Status Solidi B-Basic Solid State Physics*, (2006) **243**, 2021.
- [20] Seferos, D. S.; Trammell, S. A.; Bazan, G. C.; Kushmerick, J. G., *Proceedings of the National Academy of Sciences of the United States of America*, (2005) **102**, 8821.
- [21] Vonlanthen, D.; Rotzler, J.; Neuburger, M.; Mayor, M., *European Journal of Organic Chemistry*, (2010), 120.
- [22] Wolfe, J. P.; Ahman, J.; Sadighi, J. P.; Singer, R. A.; Buchwald, S. L., *Tetrahedron Letters*, (1997) **38**, 6367.
- [23] Lopez, O.; Maza, S.; Ulgar, V.; Maya, I.; Fernandez-Bolanos, J. G., *Tetrahedron*, (2009) **65**, 2556.
- [24] Ugi, I.; Meyr, R., *Angewandte Chemie-International Edition*, (1958) **70**, 702.

- Journal of the American Chemical Society*, (2002) **124**,  
*Journal of the American Chemical Society*, (1952) **74**, 5266.
- [27] Ugi, I.; Fetzer, U.; Eholzer, U.; Knupfer, H.; Offerman, K., *Angewandte Chemie-International Edition*, (1965) **4**, 472.
- [28] Swanson, S. A.; McClain, R.; Lovejoy, K. S.; Alamdari, N. B.; Hamilton, J. S.; Scott, J. C., *Langmuir*, (2005) **21**, 5034.
- [29] Suzuki, H., *Bull. Chem. Soc. Jpn.*, (1959) **32**, 1357.
- [30] David Vonlanthen, A. R., Artem Mischenko, Alexander Käslin, Jürgen Rotzler, Markus Neuburger, Thomas Wandlowski and Marcel Mayor, (submitted).
- [31] Kondo, H.; Nara, J.; Kino, H.; Ohno, T., *Journal of Chemical Physics*, (2008) **128**,
- [32] Huang, Z. F.; Chen, F.; Bennett, P. A.; Tao, N. J., *Journal of the American Chemical Society*, (2007) **129**, 13225.
- [33] Pauly, F.; Viljas, J. K.; Cuevas, J. C.; Schon, G., *Physical Review B*, (2008) **77**,
- [34] Henderson, J. I.; Feng, S.; Bein, T.; Kubiak, C. P., *Langmuir*, (2000) **16**, 6183.
- [35] Selzer, Y.; Allara, D. L., *Annual Review of Physical Chemistry*, (2006) **57**, 593.
- [36] Lindsay, S. M.; Ratner, M. A., *Advanced Materials*, (2007) **19**, 23.
- [37] Loo, Y. L.; Willett, R. L.; Baldwin, K. W.; Rogers, J. A., *Journal of the American Chemical Society*, (2002) **124**, 7654.
- [38] Dadosh, T.; Gordin, Y.; Krahne, R.; Khivrich, I.; Mahalu, D.; Frydman, V.; Sperling, J.; Yacoby, A.; Bar-Joseph, I., *Nature*, (2005) **436**, 677.
- [39] Liao, J. H.; Bernard, L.; Langer, M.; Schonberger, C.; Calame, M., *Advanced Materials*, (2006) **18**, 2803.
- [40] Gruter, L.; Gonzalez, M. T.; Huber, R.; Calame, M.; Schonberger, C., *Small*, (2005) **1**, 1067.
- [41] Coco, S.; Cordovilla, C.; Espinet, P.; Martin-Alvarez, J.; Munoz, P., *Inorganic Chemistry*, (2006) **45**, 10180.